Masters Program in Geospatial Technologies

Oblique UAS Imagery and Point Cloud Processing for 3D Rock Glacier Monitoring

Jordan Steven Bates

Dissertation submitted in partial fulfilment of the requirements for the Degree of *Master of Science in Geospatial Technologies*

Oblique UAS Imagery and Point Cloud Processing for 3D Rock Glacier Monitoring

A thesis submitted in fulfilment of the requirements for the Erasmus Mundus degree of Master of Science in Geospatial Technologies

At the Westfälische Wilhelms-Universität Münster

In collaboration with

Universidade Nova de Lisboa & Universitat Jaume I

Jordan Steven Bates

jbates@uni-muenster.de

Main- Supervisor

Dr. Jan Lehmann

University of Münster (WWU)

Co-supervisors:

Prof. Dr. Tillmann Buttschardt

University of Münster (WWU)

Prof. Dr. Ignacio Guerrero

Universitat Jaume I (UJI)

Declaration

I declare that this thesis entitled "Oblique UAS Imagery and Point Cloud Processing for 3D Rock Glacier Monitoring" is the result of my own research and under the guidance of my supervisors except as cited in the references. Data collected by me is genuine and was used exclusively in this thesis. This thesis has not been accepted for any degree and is not concurrently submitted in candidature of any degree.

Signature:

Name: **Jordan Steven Bates**

Place: **Münster, Germany**

Date: **24 February 2020**

Acknowledgement

I would like to thank the European Commission and the Erasmus Mundus scholarship program for the financial support and making this opportunity possible. I would also like to thank the three universities of Unisersdade NOVA de Lisboa, Westfälische Wilhelms-Universität Münster, and Universidad Jaime I for organizing the Master of Science in Geospatial Technologies program and offering the opportunity and support in helping me further my education and career. I am very grateful for having participated in this program and to the people who I have learned and drawn inspiration from.

A great amount of gratitude goes to my supervisors. To my first supervisor, Dr. Jan Lehmann, for presenting the opportunity to take up the research and map the Innere Ölgrube Rock Glacier in Austria. That is in addition to his continued support and valued insights in UAS technology and inspiration in topics. To my co-supervisor, Prof. Dr. Tillmann K. Buttschardt, for organizing and leading the data collection trip of the glacier and for collecting and providing the TLS data from 2012. Also, to his valued insights to glacier morphology, encouragement, and support throughout the process. To my other co-supervisor, Prof. Dr. Ignacio Guerrero, for accepting to support the project and help make this possible.

As always, I owe a great deal gratitude to my family and friends for their ever-enduring support throughout my pursuits.

Contents

Table of Figures

List of Tables

List of Equations

Abstract

Rock glaciers play a large ecological role and are heavily relied upon by local communities for water, power, and revenue. With climate change, the rate at which they are deforming has increased over the years and is making it more important to gain a better understanding of these geomorphological movements for improved predictions, correlations, and decision making. It is becoming increasingly more practical to examine a rock glacier with 3D visualization to have more perspectives and realistic terrain profiles. Recently gaining more attention is the use of Terrestrial Laser Scanners (TLS) and Unmanned Aircraft Systems (UAS) used separately and combined to gather high-resolution data for 3D analysis. This data is typically transformed into highly detailed Digital Elevation Models (DEM) where Differences of DEM (DoD) is used to track changes over time. This study compares these commonly used collection methods and analysis to a newly conceived multirotor UAS collection method and to a new point cloud Multiscale Model to Model Cloud Comparison (M32C) change detection seen from recent studies. Data was collected of the Innere Ölgrube Rock Glacier in Austria with a TLS in 2012 and with a multirotor UAS in 2019. It was found that oblique imagery with terrain height corrections, that creates perspectives similar to what the TLS provides, increased the completeness of data collection for a better reconstruction of a rock glacier in 3D. The new method improves the completeness of data by an average of at least 8.6%. Keeping the data as point clouds provided a much better representation of the terrain. When transforming point clouds into DEMs with common interpolations methods it was found that the average area of surface items could be exaggerated by 2.2 m^2 while point clouds were much more accurate with 0.3 m^2 of accuracy. DoD and M3C2 results were compared and it was found that DoD always provides a maximum increase of at least 1.1 m and decrease of 0.85 m more than M3C2 with larger standard deviation with similar mean values which could attributed to horizontal inaccuracies and smoothing of the interpolated data.

Keywords: *Change Analysis, Climate Change, Drone, Glacier Tracking, M3C2, Multirotor UAS, Oblique Imagery, Photogrammetry*

1. **Introduction**

Glaciers are increasingly becoming a more discussed topic as the rate they are disappearing has been increasing exponentially causing alarm because their importance within ecosystems in addition to providing evidence of climate change. According to research that combines in-situ and remote sensing techniques, the total surface area of alpine glaciers has decreased by 50% from the 1850 till 2000 (M. Zemp et al, 2006). From the same study it was predicted that it is possible that only 10% of the surface will remain in the next decade if the temperature rises by 3°C and non-existent if the temperature increases by 5°C (M. Zemp et al, 2006). Another study predicts that only 4-20% of the initial ice will be left by 2071-2100 and runoff volumes could decrease by 39% (F. Hanzer et al, 2018). These findings are alarming because of the importance glaciers have for the ecosystems and economies that surround them as well as contributing to climate change phenomena. Glaciers cover approximately 10% of Earth's land surface and have cascading impacts on downstream systems (A.Milner et al, 2017). Knowledge of glacier retreat is crucial in predicting biodiversity, biogeochemical cycles and function (R. Sommaruga, 2015). According to studies by international research at the University of Zurich, glaciers all over the world raised the sea level by 27 millimeters since 1961 Continuing to improve upon how glaciers are studied is crucial in being able to make predictions that will aid in preparedness and to make appropriate correlations for mitigation efforts (University of Zurich, 2019).

There is plethora of data acquisition methods being used and there are continued efforts in finding what works best. For acquisition, methods from high-resolution satellites imagery, Global Positioning Systems (GPS), Terrestrial Laser Scanners (TLS), Manned Aircraft, and Unmanned Aircraft Systems with optical or Light Detecting and Ranging (LiDAR) sensors are typically used (e.g., P. Nesbit & C. Hugenholtz, 2019; A. Bauer & G. Paar, 2003; T. Groh & J. Blöthe, 2019; J. Abermann et al, 2011) However, most of these data collection methods lack the ability to provide the necessary quality of data or coverage perspectives to generate a detailed and complete 3D model (A.Bauer & G. Paar, 2003). Having the ability to create a 3D model of the environment is crucial in being able to calculate the thickness and vertical wall movements of rock glaciers.

The use of TLS and UAS technology is growing within glacier tracking and geomorphic studies because of the increased quality and the ability to have on demand data collection methods (W. Immerzeel et al, 2017). UAS data has made it possible to get up to sub centimeter data on glaciers.

These systems are most used for nadir imagery using attached optical cameras while using photogrammetry to produce detailed orthomosaics and point cloud data. UAS imagery has been compared to manned aviation data collection methods where it was found to be just as accurate but with more detail (V.Kaufmann et al, 2018). Several recent studies use UAS platforms to gather high-resolution data of glaciers (e.g., W.Immerzeel et al, 2017; S. Vivero & C. Lambiel, 2019; M. Disney et al, 2019). The system used in this way misses a lot of the detail on the sides of the terrain. The use of TLS scanners are desired to gather a better inventory of rock glaciers because of their ability to capture angles often missed from traditional remote sensing means (K. Krainer et al, 2012). Bauer & Paar (2003) express how the front slopes of a rock glacier change often and partially due to falling debris in which they use a TLS in their studies to capture the front and sides in enough detail to monitor this. TLS data delivers good coverage of the sides because of the horizontal perspectives it has from the ground and if positioned correctly with a nearby hill, coverage of the top of the glacier can be obtained. However, with TLS it is difficult to place the scanner in enough locations to avoid data gaps or missing coverage especially rugged terrain such as rock glaciers (Fugazza et al, 2018) However, Fugazza et al. (2018) decided to integrate UAS to capture the occlusions or missing areas left by the TLS data. Additional studies concerning Alpine terrain have also taken advantage of using the combination of UAS and TLS methods for complete coverage in which the left side of Figure 1 depicts (J. Šašak, 2019). Multirotor UAS are commonly used in many sectors such as real estate to fly from oblique angles to gather data on the facets of houses to create complete 3D model (F. Remondino et al, 2019). Practices of using multi rotor UAS to capture information on the sides and face of glaciers like this are rare or simply non-existent. Such practice could be beneficial especially with photogrammetry having the potential in being just as or more accurate than LiDAR solutions (J. Ryan et al, 2015).

Even if the data collection method provides improved perspectives around the entire environment, many of the ways analysis is being done and the data structures being chosen reduces or nullifies these benefits. Most of the glacier studies found transformed their data to DEMs (e.g., D. Fugazza, 2018; M. Disney et al, 2019; W.W. Immerzeel, 2017; E. Schwalbe et al, 2008) which are considered 2.5D rather than 3D with only displaying average height values in a 2D raster. These transformations decrease the benefits of any increased perspectives of the sides.

Photogrammetry derived point clouds have increased with the increase use of small consumer multirotor UAS platforms (Remondino et al., 2018). Point clouds are the preferred 3D data structure of choice and is considered survey grade because of its ability to represent the environment with precision and no interpolations. An open source software called CloudCompare is being used in several recent studies to process point clouds along with computing differences between them. Instead of transforming the data into a DEM, Bash et al (2018) uses one of the newer point cloud processing methods called Multiscale Model to Model Cloud Comparison (M3C2) to process his UAS surveys. Vivero and Lambiel (2019) also use M3C2 in attempt to provide a better representation of the surface roughness in a change analysis.

There is a need to further explore advancing technologies such as with flight characteristics of multirotor UAS to benefit the data collection and the capabilities of point cloud processing to gain and maintain the most information about the reality of glacier surfaces and movement. This study applies the advantages of multirotor UAS with data collection flight paths and angles typically not employed for rock glacier studies as can be seen in Figure 1. It will compare the performance of this method in reconstructing the 3D glacier environment as compared to current high-resolution 3D collections methods from nadir UAS flights, TLS scanning, and the combination of both. The study will use the M3C2 point cloud processing method to do change detection between a TLS point cloud from 2012 and a UAS point cloud from 2019 of a rock glacier. The two data sets are converted into DEM's where Difference of DEMs is performed. A comparison of the DEM and point cloud data and their corresponding change analyses are made to understand how they differ in providing results and accuracies. This study will shed light on the possibility of multirotor UAS systems being a singular set of equipment for a complete 3D collection method while examining the use of point cloud as the chosen means of analysis for monitoring rock glacier movement.
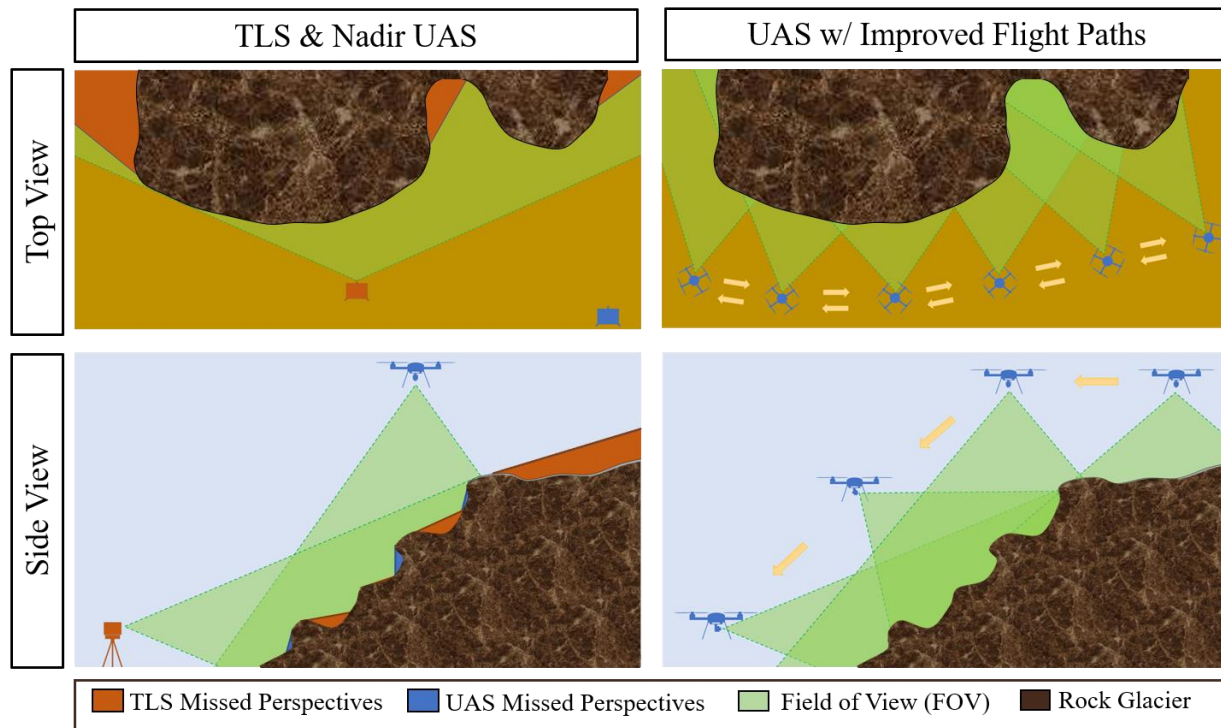
Figure 1. Illustrating possible perspective gains using the advantages of multirotor Unmanned Aircraft Systems (UAS) flight capabilities and oblique imagery in place of a Terrestrial Laser Scanner (TLS)

1.1. Aim and Objectives

Based on past research, there is indication that UAS photogrammetry derived point clouds can be just as accurate and detailed as TLS point clouds. However, TLS and terrestrial photogrammetry are still desired to get perspectives of sides that UAS and other aerial and space platforms have not been able to gather. In either case, many studies are exploring the ability to avoid interpolations and use point clouds for glacier analysis. The question arises, can multirotor UAS be used to capture oblique imagery from perspectives that would lessen the need for TLS equipment? In addition, since DEMs are popular but posed as providing less detail and accuracy, how different are transformed DEMs to their initial point clouds? How will these differences carry over to the change analysis methods of each data type? With this the following objectives were derived:

1. Compare and quantify the coverage difference between TLS scans, UAS nadir imagery, UAS nadir imagery integrated with the TLS scans, and UAS nadir with terrain corrected oblique imagery.
2. Observe how the TLS and UAS point clouds are affected when transformed into DEMs
3. Observe the difference in DoD and point cloud change methods

2. Materials and Methods

2.1 Study Area

The Innere Ölgrube Rock Glacier located in Kaunertal, Ötztal Alps, Austria was used to examine the collection and processing methods presented in this project. The location and an aerial overview of the glacier can be seen in Figure 2. This area is a central Alpine valley that consists of approximately 129 rock glaciers (T. Buttschardt et al, 2012). The mean air temperature for this area is between 0 degrees Celsius and -1 degrees Celsius with the temperatures having increased by approximately 1 degree from 1935 to 2010 (J. Czempinski, 2017). F. Hanzer (2018) and his associates used a physically based hydro-climatological model to asses future climate change impacts on the Otztal Alps and found that the temperature could increase up to 2.2 degrees within the next century (F. Hanzer et al, 2018). With these temperature increases, it is predicted that the glacier presence in this area will decrease significantly. Total glacier volume in the area could likely decrease 60-65 percent until 2050 and 80-96% by the end of the century (F. Hanzer, 2018)

The Innere Ölgrube rock glacier is derived from metamorphic rocks consisting of blocks several meters in length (K. Krainer et al, 2006). It is characterized by having two tongue-shaped lobes with a width of approximately 400 m and a length of 880 m (K. Krainer et al, 2006). The base of the face of the glacier is at an altitude of 2380 m with its head extending to approximately 2800 m creating a very steep gradient of around 40-45 degrees. On the right side of Figure 2, it can be seen that rock glaciers like this have very complex surfaces with large variations in slope and ruggedness with transverse and longitudinal ridges and furrows along the top surface (K. Krainer et al, 2006).

Past studies have examined the movement of the Innere Ölgrube rock glacier. In a study by K. Krainer and X. He (2006), rocks on the surface were marked and tracked using Dual GPS (DGPS) to estimate the movement. It was found that the glacier from July of 2002 to July of 2003 had moved at a maximum of 1.36 meters and a minimum of 0.09 meters. The most movement occurred in the center areas nearest to the face / front of the glacier while movement decreasing towards the edges and back. The more recent study performed by T. Groh and J. Blothe (2019), calculated movement using aerial survey data from 2001 to 2018. They found that the glacier's mean annual surface velocity is 0.5 meters with the most movement occurring closest to the northern side of the

face of the glacier. With these results it was expected to see the most movement near the northern portions around the face of the glacier with ranges anywhere from 0.5 m to 1.36 meters a year. However, neither of these studies provided information about the movement of the face or sides of the glacier and only provide insights on the top surface.
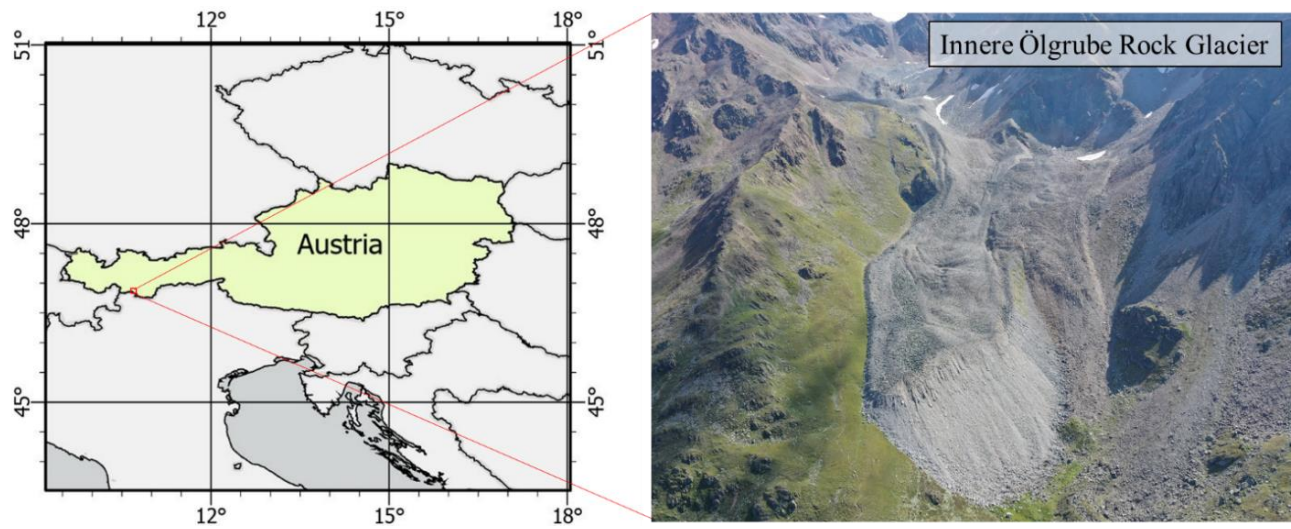
Figure 2. Location of study area in the Kaunertal Valley, Austria and 2019 UAS aerial view of the Innere Ölgrube Rock Glacier.

2.2 Data Collection

Data used in this project was collected from a TLS in 2012 and a small UAS in 2019. The University of Münster had collected TLS data in the past while data was recently collected in September 2019 using a multirotor UAS. Both these means of collection made it possible to reconstruct a 3D point cloud from the past and the present with more perspectives than just the top surface. Because of these acquisitions, this study was able to compare both 3D data collection and change detection methods with perspectives of the glacier that are not often examined. An overview of the data collection is visualized in Figure 3.
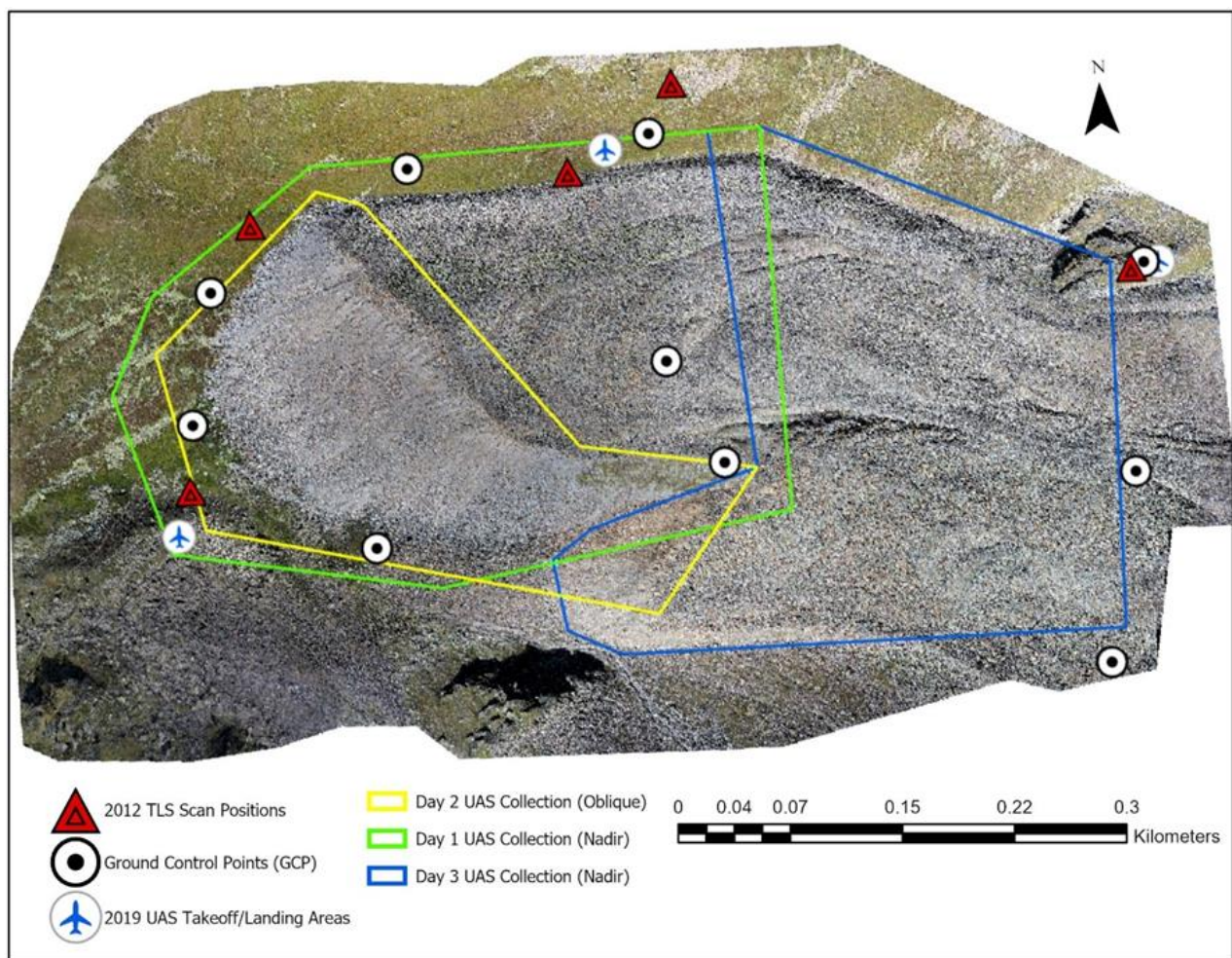
Figure 3 Depiction of the data collections that took place. The 2012 TLS scan position in association with the 2019 UAS flight coverages of each day along with the associated take off points and Ground Control Points (GCP) used for georeferencing.

2.2.1 TLS Acquisition (2012)

The TLS used to collect the 2012 data was the Optech ILRIS-3D. TLS is a ground-based LiDAR technology system. A light beam is emitted by an active transmitter which is then reflected by the targeted object. A photodiode acts as a receiver where part of the back reflected light is registered. The time from transmission and registration is used to calculate the distance (T. Buttschardt et al, 2012).

The scanner's specifications can be seen below in Table 1. Since the scanner's range is from 3m to a maximum of 1200m, it is capable of capturing the extents of the rock glacier being studied considering it is at the appropriate perspective angle. The whole system is comprised of a tripod, turn-tilt base, handheld computer, sensor, and batteries. The scanner weighs approximately 13 Kg aside from the tripod and other accessories and took a minimum of 2 individuals to carry up to the study area.

Table 1 Specifications of the scanner used and collection statistics from the project

TLS System Specifications		
Sensor	Optech ILRIS-3D	
Min. Spot Spacing	2 mm	
Max. Range	800 m	
Accuracy	8 mm	
Sensor weight	~13 kg	

2012 Data Collection Statistics	
Collection Time	3 Days
Scan Locations	5
Scans	36
Data Storage	1.14 GB

Figure 4 Overview of the 2012 TLS scanning positions on 3D model of the rack glacier for illustration height and perspective differences

The 2012 expedition took place from July 16 to July 22 of 2012. Three days were used for data collection where it was made possible to complete scans from five different locations. As can be seen in Figure 4, the scan locations took place with Scan 01 in front of the face of the glacier with scanning from the north-east to south-east direction, another with Scan 02 to the side of the face with scanning to the southeast to southwest directions, the two with Scan 03 and Scan 04 at the side of the glacier with scans in the southeast to southwest directions with scan 4 being farther away and at a higher altitude creating the ability to capture parts of the top of the glacier, and scan 5 being at an elevated part of the glacier to once again capture more of the top portions of the glacier with scans in the west to south directions (T. Buttschardt et al, 2012). The scans were executed in a manner in that each adjacent scan or more would overlap having several common features to use as reference points to align the scans. These reference points would be large exposed boulders or obvious and particular topographical zones that would be easy to identify in each scan. However, it was discovered later that there were two damaged data records from scans 02 and 03

causing a lack of reference points in those areas for scan alignment and registration. The focus of the previous study was the face of the glacier to derive the slope for determination of glacier activity and because of this, the most complete areas of collection are at the front of the glacier.

2.2.2 UAS Acquisition (2019)

The most recent data from 2019 data was collected using a small Unmanned Aircraft System (UAS). The collection expedition took place from the August 30 to the September 4 of 2019. Like the TLS collection in 2012, three of those days were used to collect mapping data of the rock glacier. The UAS that was used was a DJI Mavic 2 Pro which is a common consumer system because of its size, sensor quality, and price. The equipment used included a hand controller, four batteries, and the aircraft itself with an already integrated camera while using a Samsung Galaxy S8 in conjunction with the hand controller to interface with the aircraft. The whole system weighs an approximate 0.9 kg and was able to fit in a small carrying case with dimensions of 60cm x 30cm x 20cm needing only one person to carry it. It has a maximum flight endurance up to 31 minutes, flight range of 18 km, and a 1 inch Hasselblad camera as the sensor with 20 megapixel resolution.

The flights were planned using DroneDeploy's online UAS flight software and to be consistent with the extent of the area covered by the past TLS scans in 2012. Keyhole Markup Language (KML) files, tracing the extents of the past collection, were imported into the software. The software provided estimates of battery expenditure based on the flight parameters selected. With four batteries available, it was possible to get approximately two hours of flight time a day and those areas planned and mapped of the glacier each day can be seen in Figure 3.

The plan was to first capture the front to midway up the glacier on the first day, then to capture more information of the face and base of the glacier on the second day since this was the most important part, and to capture the rest of the glacier on the third day. The flight profile chosen for day 1 and day 3 was from the generic 3D data collection option within the software that offered double grid flight lines for the nadir imagery with oblique imagery being captured around the edges of the planned flights with the camera looking inward to the center of the flight boundaries. This method is the recommended setting when gathering data to develop a 3D model and has been proven to produce improvements in past studies (P. Nesbit & C. Hugenholtz, 2019). The double grid or cross hatch flight path has the aircraft fly in a typical grid, flight lines back and forth as if "mowing the lawn", then flying those same type of lines and extent but perpendicular to the

previous grid lines. This allows the sensor to capture the environment from more directions to better characterize the environment. The oblique flights at the end of the automated flight profile edges would have the camera-orientation inwards with the camera angle at 65 degrees from the ground to better capture the sides of the glacier.

The flights were planned to be at a height of 46 meters above ground which gave an image resolution of approximately 0.4-0.5 cm Ground Sampling Distance (GSD). Each flight line and image capture were based on an image overlap of 70% forward and 75% side image overlap. The resolution fluctuates slightly due to the variation of the terrain and steepness of the Alp and glacier. The aircraft maintains the flight altitude in relation to the take off point. This was taken into consideration when planning the flight altitude and take off area. To provide context of the steepness and amount of altitude change of the glacier, the glacier increases from 2404 meters high to 2780 within its 800 m length. The software at the time, like others compatible with the Mavic 2 Pro, did not have the option for the altitude to automatically correct for terrain height changes during the automated flight profile for a consistent GSD. In an effort to compensate for this, flight sections were planned at different heights as can be seen in Figure 5. Geographic Information Systems (GIS) such as ArcGIS Pro ang Google Earth Pro were used to check terrain profiles, heights, and characterize the surroundings for situational awareness aided in determining the best flight altitude for the area. More flight sections with different altitudes could have been created to better adapt to the slope but with sacrifice in collection efficiency and battery performance. It was planned to take off the aircraft at the highest point inside the flight mission extent so that the 46 m altitude would be safe at the upper limits in that flight grid while this altitude was low enough to still provide good quality for the rest of the downslope areas.

Table 2 Specifications of UAS used and the collection facts from this project (fix font of table and expand specs and info)

UAS Specifications	
UAS Platform	DJI Mavic Pro 2
Sensor Resolution	20 MP
Weight (kg)	0.9
Dimensions (mm)	214 × 91 × 84
Max. Flight Distance	18 km (@ 50 km / h)

2019 Data Collection Information	
Collection Time	3 days
Number of Flights	7
Nadir Image Count	1,185
Nadir Image Storage	16.3 GB
Nadir + Oblique Image Count	3,355
Nadir + Oblique Image Storage	41.2 GB
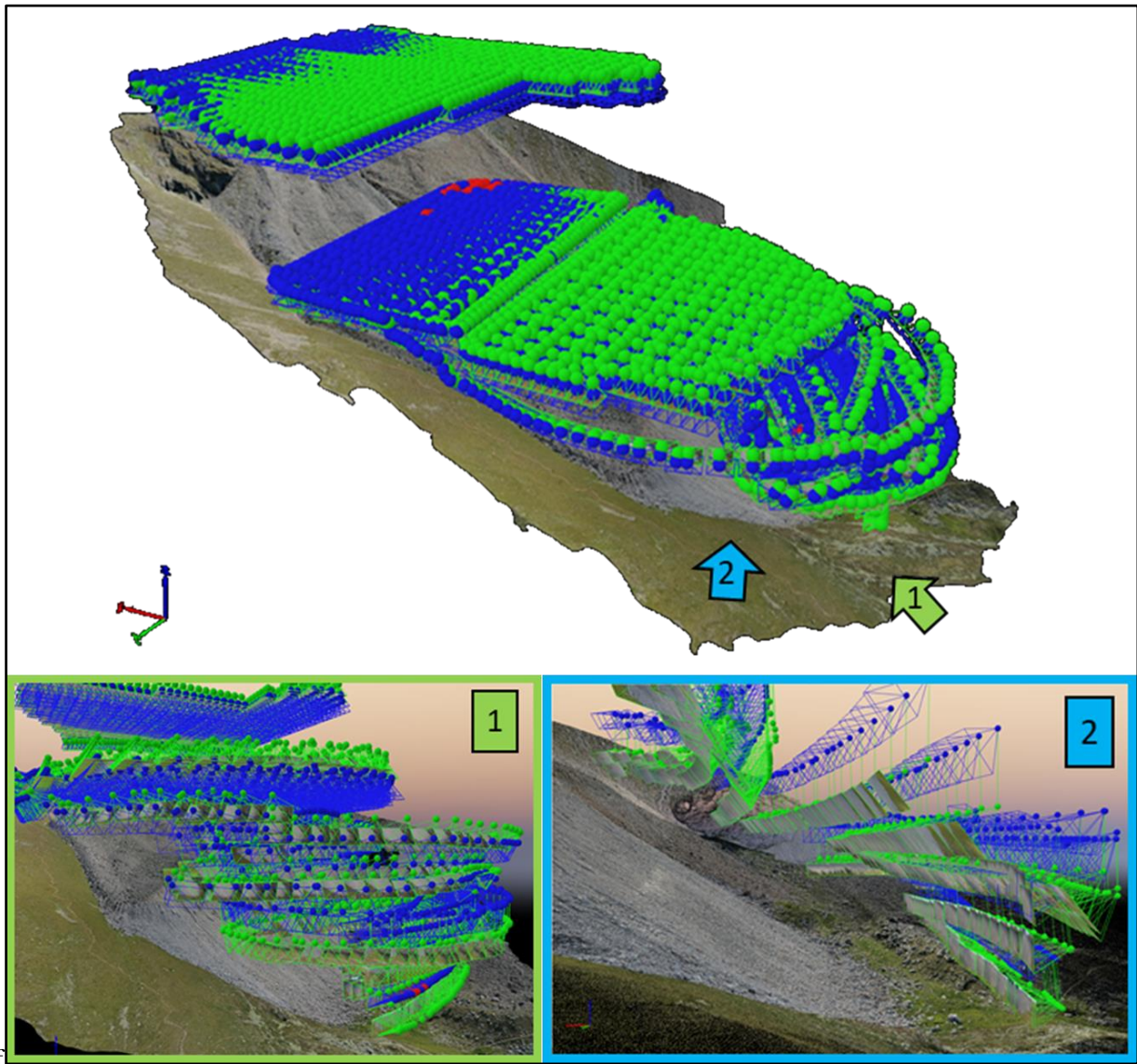
Figure 5 3D view of UAS image captures with windows 1 & 2 displaying the oblique and terrain corrections at the face of the glacier that provided perspectives similar to a TLS

Day 2 was focused on oblique imagery at the face of the glacier. There is currently no flight planning software available for any DJI UAS to plan an automated oblique flight from one orientation at varying heights and camera angles for a single irregular facet like a cliff. The flights at the face of the glacier had to flown manually. DJI offers a flight mode to select a Point of Interest (POI) of interest during flight while being able to establish the radius from it and flight altitude and orbit direction. Using this it was possible to semi automatically fly a nonhorizontal grid mission. These methods were used while trying to maintain a consistent distance from the face of the glacier and changing the angle of the camera until it was near the perspective of the TLS. On the lowest point of the flight the camera captured an angle of nearly 120 degrees from the nadir position or 30 degrees up from the ground. This type of flight was performed in hope to gain perspectives similar to the TLS while also providing the typical perspectives from a UAS.

For operation of the UAS, DroneDeploy's phone application was used as the Ground Control Station (GCS) software for automated control of the UAS. Those flights planned on the computer were able to be seamlessly accessed and used from the phone in the field. A total of 9 flights were performed. From the data that was captured, the nadir images were extracted to be isolated. This way the nadir images could be processed alone after being processed with the oblique data. This will be used to compare what improvement if any are made when the oblique imagery is added to the nadir imagery. A total of 3350 (45.6GB) images were taken with 1102 (15.2 GB) of those being the nadir images.

2.3. Data Processing

The processing steps used in this project focused on preparing the data from the past and present in a way that can be fairly compared and used in a change analysis. The workflow needed to achieve the objectives in this project can be found in the flow chart of Figure 6. The GPS data that was collected in 2019 was converted to the same coordinate reference system as the UAS data, World Geodetic System (WGS) 84 Universal Transverse Mercator (UTM) zone 32N (EPSG:32632). The GPS data was used to georeference the 2019 UAS data during the photogrammetry processing and to assess the Root-Mean-Square Error (RMSE) of the data sets. The TLS data was processed using CloudCompare for scan registrations while the UAS data was processed using photogrammetry within Pix4D. Once the processing of the point clouds were complete, the data was consolidated in CloudCompare where the rest of the point cloud editing

took place. The 2012 TLS was aligned and registered with the georeferenced 2019 UAS data for local and global alignment. It was further cleaned up and segmented to the same extents. Once the data sets were matched in geolocation and extent, they were rasterized both in the Z dimension and X dimension, with Z providing the perspective from above the study area and X providing the view in front of the glacier's face for a multidimensional view. In the rasterization process, cells with no value due to lack of data coverage could be calculated. This made it possible to quantify the completeness achieved by the collection method from that particular dimensional view.

The point cloud data of the glacier face from each collection method was transformed into DEMs using various interpolation types within ArcGIS Pro. Only the front of the glacier was chosen because of alignment issues that occur when using the entire glacier extent from the 2012 data. In addition, the sloped glacier face is the most important of all because of the studies interest in data completion, processing, and change detection on hard to reach near vertical surfaces. The next part of the analysis, compared measurements made within DEMs and point clouds to understand the accuracy or differences among the data types and collection methods. The DEMs were then used for Difference of DEM (DoD) change analysis between 2012 and 2019 to see how the different interpolations affect the outcomes of the results. The point clouds with the same portions of the face of the glacier were used to do a change detection using the newer M3C2 algorithm.
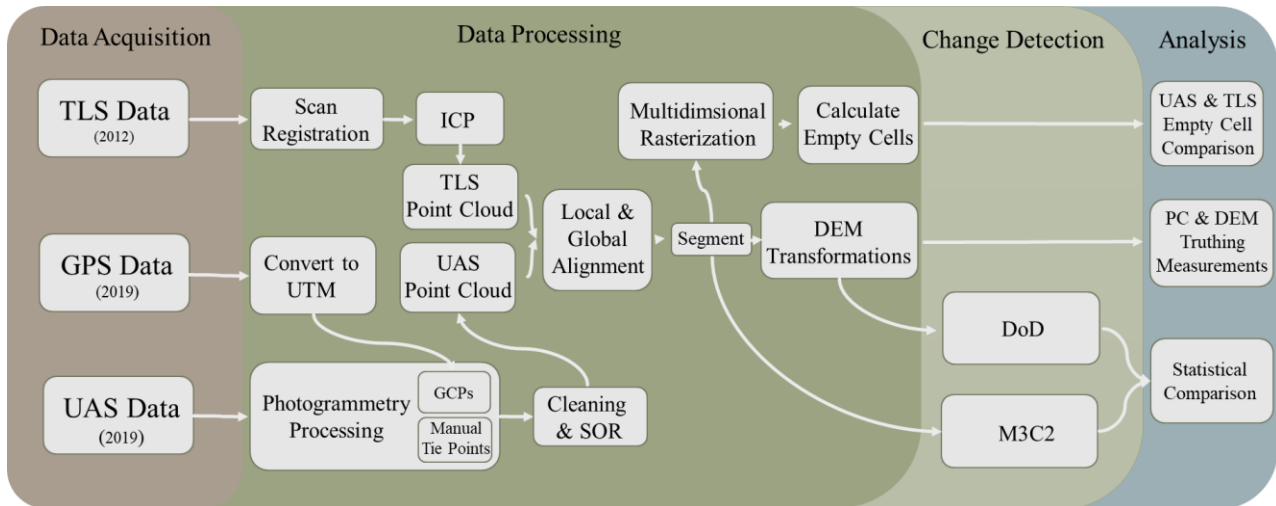
Figure 6 Flow chart depicting the overall methodology of this project with data collection methods, the processing steps taken, and the analysis performed

2.3.1 GPS Data Processing

The GPS data was collected using a DGPS with the data being marked on top of GCP points spread across the study area. The data was organized and visualized using QGIS where it was then converted to WGS 84 UTM zone 32N (EPSG:32632) and then exported into a Comma-Separated Values (CSV) file. The UAS GPS data was incorporated using Pix4D's GCP manager while processing the imagery.

2.3.2 TLS Scan Registration and Processing

Each of the five scanning locations were comprised of individual sections. Typically, each scanning location was comprised of 3-6 sperate parts because of varying areas of interest. Each of these sections and scanning locations needed to be aligned. Every section had overlapping features that could be used as reference points to complete the alignments. However, three files were corrupted and unable to be used which made it difficult to have enough reference points to align the top parts of the glacier. This problem is reflected later with in the RMSE results seen in Table 3. In the past it wasn't possible to align the top sections because of the damaged files but with the current 3D model from the UAS for reference in CloudCompare the scans could be initially oriented in the correct manner. The steps taken to reconstruct a 3D model of the rock glacier with the TLS point cloud data can be seen in Figure 7.
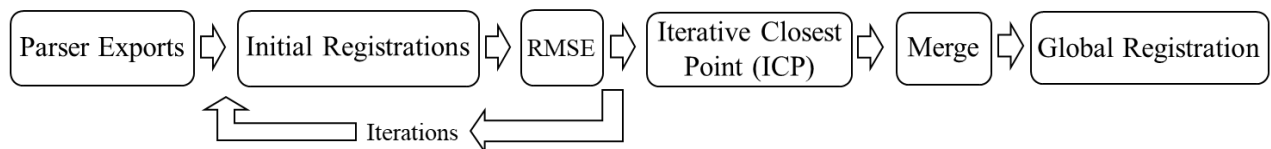
Figure 7 Workflow for construction of 3D point cloud model derived from TLS data

All individual scans were preprocessed and exported into the appropriate file format using the Optech Ilris 3D Parser software. Once each scan was oriented using the current UAS glacier 3D model as reference, the initial registration of each overlapping scan was performed with manual alignments. Large rocks that stood out or obvious land formations that were shared by overlapping areas were used to align the individual scans. In Figure 8 it shows the overlapping complexity of the scans and an example of one of the reference points used illustrating how meticulous the matching process can be. Four to eight pairs of matching points were used for every section with

multiple iterations of alignment taking place. There were 24 scans meaning that there were at least 48 reference points used which can be time consuming especially with multiple iterations.
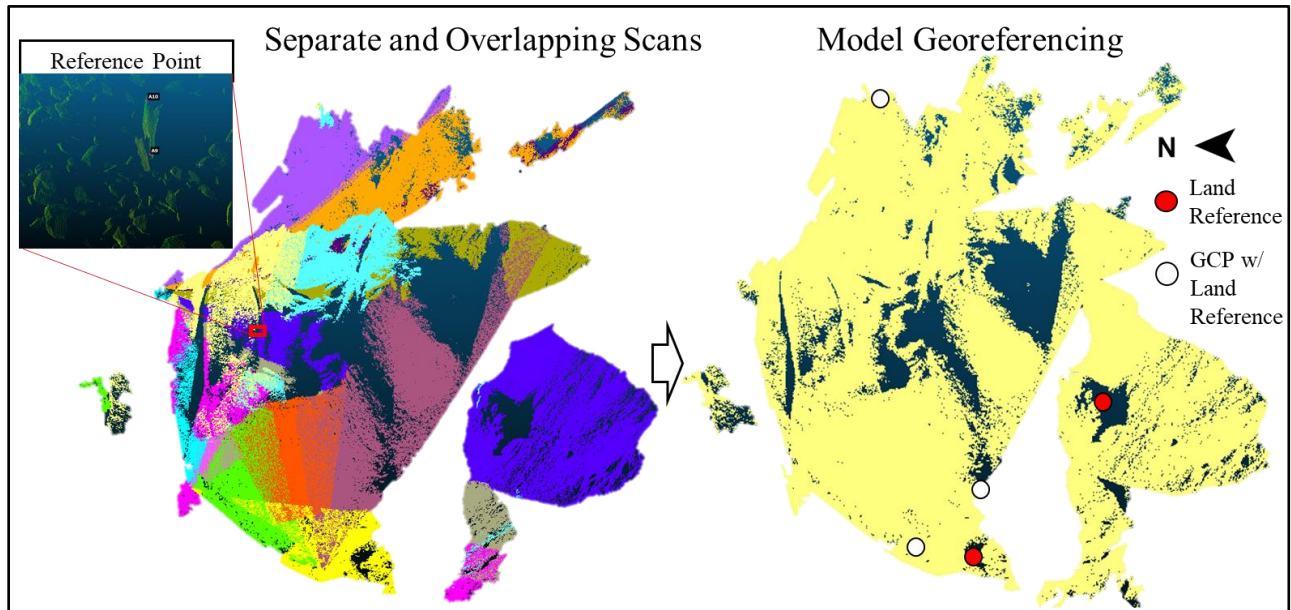
Figure 8 Illustration of an example of one of the large boulders used as one of the many reference points along with a depiction of the amount and locations of the overlapping scans in the project. The rights side shows the location of terrain and GCPs used for georeferencing once the scans were merged

Table 3 Table showing the average errors in alignments from each scan position along with the global georeferencing errors with the all scans combined and with only scans on the face of the glacier combined

Registration Info		Registration Scan Matching Errors		Global Registration with 2019 GCP Data	
Registered Scans	24	Scan Position	RMSE (m)	Combined Scans	RMSE (m)
		1	0.12		
Processing Time	20 hours	2	0.14	All Scans	5.1
		4	0.08		
Model Storage	1 GB	5	0.89	Glacier Face	0.7
		Average	0.31		

After the initial alignments, Iterative Closest Point (ICP) matching was used for finer registration. According to A. Fuad's (2018) findings in his study, ICP was the most suitable way of registering point clouds with mobile laser scanning data (N. Ahmad Fuad et al, 2018). The ICP matches one point cloud with another using Euclidean space and calculates the appropriate rotations and translations needed for alignment while minimizing a distance metric between each point (N. Ahmad Fuad et al, 2018). Most sections would overlap by approximately 10% so this was the setting that was chosen in the tool. The tool recommends that the smaller the overlapping the better

the initial registration should be before running ICP. An RMSe value of 10^{-8} was used as this was found to achieve the optimal result in a similar use case. (S.Vivero, et al, 2019). In Lague's study he found that ICP did not work any better than manually matching points but that ICP only works well when the scan is highly detailed with high point density (D. Lague, 2013). In some cases it did not improve the matching especially on the top surface of the glacier at areas with prominent data gaps. The construction of the model took approximately 20 hours to complete.

Once the registration of the scans achieved the highest RMSE of several iterations of the process, the scans were merged together. Two models were created with one being just the scans of the face of the glacier and another being the entire extent. These models were then georeferenced by being aligned with the 2019 UAS data. Notable land features such as surrounding cliffs and boulders with some being where GCPs were placed were used to register the scans. The location of these features with those that were marked with a GCP can be seen on the right side of Figure 8. The model of just the face of the glacier was able to be matched with a RMSE of 0.7 m based on the alignment of the features. The model of the entire glacier was matched at a much higher RMSE of 5.1 m. This much larger error could be attributed to the decrease in matching quality of the scans on the top of the glacier with there being more scans and with less overlap because of damaged files.

2.3.3 UAS Photogrammetry Processing

The imagery from the UAS was processed into a point cloud using photogrammetry and computer vision processes within Pix4D. Photogrammetry is the process of deriving metric information about an object through a measurement in a photograph (M. Pepe et al, 2018). Two or more images are used together where lines of sight (rays) can be intersected on the object to create a triangulated position on points of interest. In order for the object to appear in multiple images, a method of overlapping the images on all sides (side and front overlap) during collection were used. The change in position of object in the view in relation to the sensors position is the parallax (M. Pepe et al, 2018). So that information about the side of features are captured, oblique images from the sides are taken of the environment instead of straight down nadir images. Photogrammetry software uses topology within the color textures and abrupt changes from edges to locate these points as they change position in each image which is where computer vision intersects with modern photogrammetry (I. Colomina, 2014).
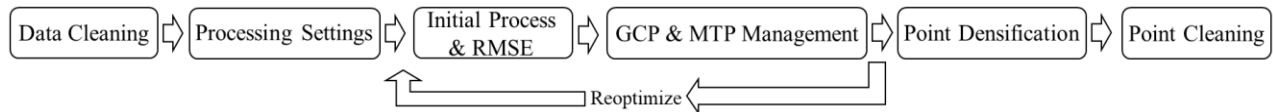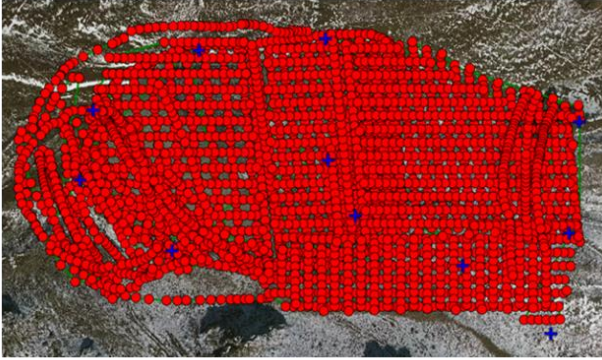
Figure 9 Workflow used to process the 3D point cloud from the UAS data

The workflow used in this project for processing the UAS data can be seen above in Figure 9. The first step was to clean the data from examining the images collected and clear out repeated, blurry, and other photos harmful or unnecessary to the quality model. On turns, there are typically photos that are not needed or repeated because the rotor aircraft is pivoting around in the same spot while the camera is still taking photos. At times when the aircraft rotates too quickly on turns or the aircraft is closer to the ground at certain points in the flight, blurriness could occur both from camera focus and aircraft speeds. This was an experienced problem with mapping the glacier because of the rapidly changing topography. However, only six images were affected this way and were deleted for lack of necessity to help processing efficiency and to maintain quality.

There were two sets of photo groups created from the data collected in order to process two different models. One featured all the flight characteristics and elements that are recommended for better 3D models with the cross hatches and oblique imagery around the sides with the addition of the unique flight perspectives on the face of the glacier being used in this project. The nadir and oblique images combined totalled 3350 images. The other group were only nadir imagery with those resembling a typical hatch flight path in a single bi-directional pattern which is the most common in UAS mapping as seen in the image of Table 4. The nadir images alone totalled 1185 image. These will later be used to compare the impacts of added 3D collection methods.

Table 4 Comparison of processing specifications and results between the UAS nadir (only) and with the UAS oblique and nadir (combined)

UAS Nadir	UAS Nadir + Oblique

Processing Info & Results		Processing Info & Results	
Processing Setting	Rapid ¼ Scale, Low Point Density	Processing Setting	Rapid ¼ Scale, Low Point Density
Processing Time	2:05h	Processing Time	3:33h
Model Storage	158 MB	Model Storage	530 MB
Resolution	2.28 cm	Resolution	2.27 cm
Avg. Point Density	45.26 m^2	Avg. Point Density	91.6 m^2
RMSE	1.02m	RMSE	1.8 m

When processing the data the following settings were used in Pix4D:

Keypoints Image Scale: Rapid (1/4 Image Size)

Point Cloud Densification Image Scale: Rapid (1/4 Image Size: Multiscale)

Point density: Optimal

Minimum Number of Matches: 3

Selections for faster processing speeds were used because of a limited time frame with the Pix4D software licensing. Both image groups were processed with the same settings for consistency. The *Keypoint* matching is the setting for the initial processing step in which common points within images a created for matching and structuring the model (Pix4D, n.d.). The additional parameters were for the next step in processing and the creation of the point clouds. *Point Cloud Densification Dmage* scale options are used to set which scale the images will be when computing addition 3D points around the keypoints. Multiscale allows it to use multiple image scale less than the one

chosen. The point density parameters determine the density of the point cloud. For every 4/ image scale pixel a 3D point is computed with the optimal setting chosen. In this project a point was computed (4/0.25) every 16 pixels of the original image (Pix4D, n.d.). Minimum number of matches option sets a threshold for every 3D point in that they each must have been correctly re-projected from at least the number images defined by the user. Settings for the camera did not need to be managed as settings for most DJI aircraft sensors have already been integrated in the Pix4D software and is recognized by the software from the image metadata and the appropriate settings are automatically created.

Once the initial processing stage is over, an initial report is made and those 3D keypoints that were generated can be viewed in the Raycloud window. The initial report displays the results of the image matching, the projected average Ground Sampling Distance (GSD), and RMSE's. Ground control points were added using the Raycloud viewer. While inspecting the Raycloud, it was noticed that there was misalignment along the front of the glacier in the model with the integrated oblique imagery. This is theorized to be because of the drastic differences in camera angles along the front of the glacier as this was not an issue with the model with the nadir imagery only. Manuel Tie Points (MTP) were created to help define what locations in the images were the same because these locations changed between the photos more with the increased angles and altitude changes. This helped aid the computer vision process in reconstructing and adjusting the model. An example of manually selecting the image points for the MTPs and GCPs can be seen in Figure 10.
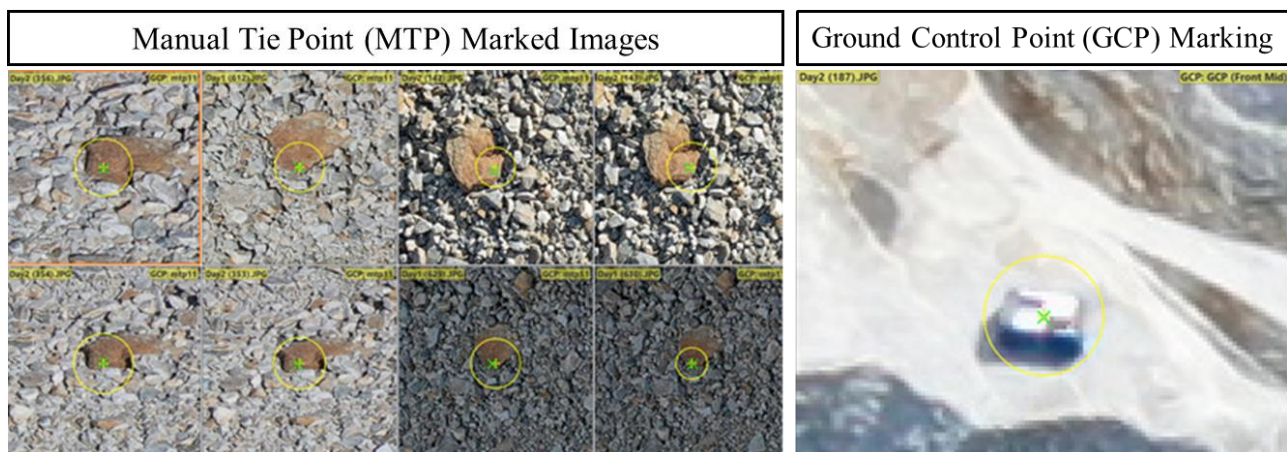
Figure 10 (Left) shows an example of a MTPs being placed on the same object in each image and (Right) shows an example of one of the GCPs being marked in the Pix4D environment

MTP markings were spread across the front and middle of the glacier to try and define a good coverage of common points across the model and where the misalignment appeared to be happening the most. GCPs were placed, as stated before, around the edges of the glacier with some being in the middle for a well fitted georeferencing with no skewness. The distribution of these points can be seen in Figure 11. The initial model was on average 30 meters below the actual elevation before the GCPs were used as can be seen in Figure 11 as well. This illustrated the importance of their use as the georeferencing from triangulation of the UAS's GPS provided Z values that were significantly off.
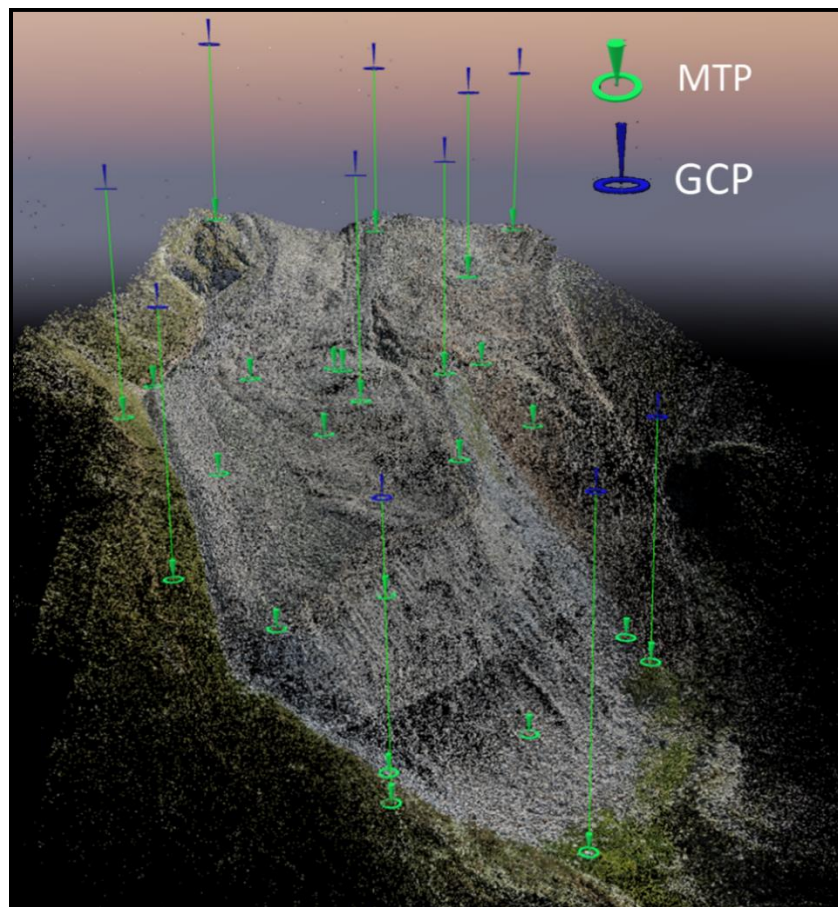
Figure 11 Showing the distribution of MTPs required to appropriately align the data from images varying from many angles and altitudes and the GCP placement across the rock glacier

The model was then reoptimized to integrate the new tie points from MTPs and GCPs. After the point cloud was densified and exported, it was imported into CloudCompare. The additional caveat of the oblique imagery at the front of the rock glacier is that it caused increased noise at the top edge of the face. The lowest row of images taken at the base of the glacier have some sky and

clouds in the images. The noise consists of white and blue points which indicates that the noise was created because of the inclusion of the sky and clouds from the camera angle used. The tool' "Statistical Outlier Removal (SOR)" was used to remove these points. SOR computes the average spacing between the points and will reject those points that are farther than the average spacing from any other point plus a user defined number of times the standard deviation (CloudCompare, n.d.). The noisy points above the face were sporadic with much larger spacing than the actual surface points. Three times the standard deviation was used in order to prevent removing any surface points.

Two photogrammetry 3D point cloud data sets were created. One with nadir imagery only and the other with both nadir and oblique imagery to use in comparison in this study. The resulting models statistics for resolution, accuracy, and processing times can be seen in Table 4.

2.3.4 Preparation for Temporal Data Comparison & Testing

Steps were taken before doing the rasterization, interpolations, and change testing to ensure the data sets from 2012 and 2019 were appropriately aligned and set to the same extents. This was detrimental for the coverage testing to define the same extent around the glacier so that the coverage percentages of the glacier surface are in relation to the same areas. For change testing it was desired to have the best fitting models of both years for the most accurate change detection.

The alignment was checked with five known and fixed locations on the map. Features were large unmoving boulders and cliff edges, and some were locations where GCPs were placed. As mentioned before, the RMSE of aligning the entire glacier was 5.1 meters as compared to the 0.7 meters when just matching the fronts of the glacier. This is most likely due to some of the missing scans on the top along with this area having more smaller scans that needed to be aligned with allotted and propagated small errors in matching and alignment in the registration steps. It was decided that the whole glacier could still be used for data completion comparisons of the collection methods but would not be used for change detection with the high RMSE. The front would be used for the change detection testing which is also beneficial in the fact that the TLS data was more complete at the front.

After both the point clouds were checked for alignment, a polyline was drawn around the extends of the glacier. One was created for the entire glacier while the other was created around the face

of the glacier. These polylines were then used for segmenting out the desired extent. The TLS cloud was used as a reference to draw the polyline for the face of the glacier as it was less complete on the southern sides. With the amount of missing data on that side, it was decided to avoid it because the adverse effects it would have on the change detection. Figure 12 shows the polyline used to clip out the face from both data sets. The whole glacier segmented part will be used in the completeness comparison. Whereas the front section was used for both the completeness comparison and change detection analysis as it was more complete and accurate.
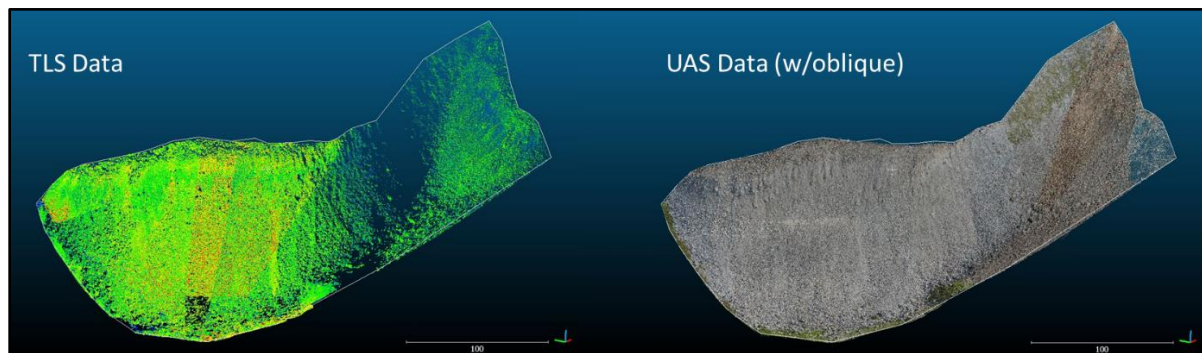
Figure 12 Illustrating the same polyline used to accurately segment the identical extents of the data portions being examined which in this case is the face of the glacier

2.3.5 Rasterization of Models

This processing step was used in order to produce results that quantify the completeness of the data collection methods used. These results were used to compare the performance of the 2012 TLS collection and the 2019 UAS nadir data separately and combined against the 2019 UAS nadir plus oblique data. The segmented face of the glacier and the full glacier segmentation models were rasterized using CloudCompare. This process converts the 3D information into a 2D raster with the pixel values being defined by the point values that fall inside the pixel dimensions (CloudCompare, n.d.). The direction of the model or dimensional plane chosen will determine the orientation of the 3D model when the grid is overlaid on the points to determine the pixel values. The X and Z dimensions were used. The Z dimensional perspective provided a view from straight above and X provided a view directly in front of the glacier's face as seen in Figure 13.
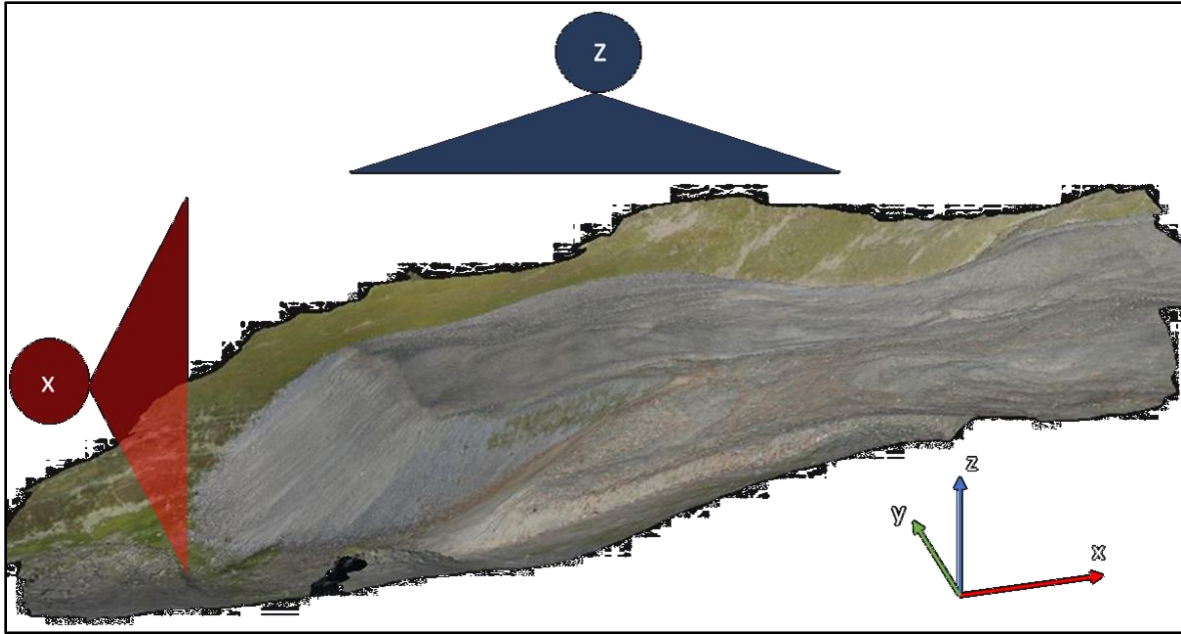
Figure 13 Illustrates the perspectives from which the data was rasterized to offer a quantification of data completeness three dimensionally

These perspectives would provide insight on how much each data collection covered the top of the glacier while also gathering information on a near vertical plane such as the most important, the face of the glacier. A setting was used to have those cells with no point values within their dimension to be set at void/null. Raster cell that fell outside of the study area after rasterization were removed and raster calculations were used to determined what percentage of cells were left empty within the original segmented areas. Practically this allows for a way to quantify the amount of coverage gathered of the glacier multidimensionally by each collection type.
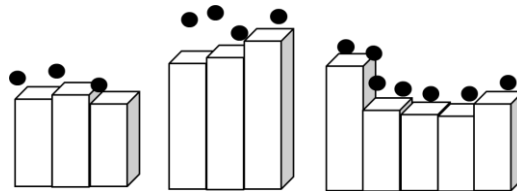
Figure 14 Depiction of how the raster cell height values are determined by point data within their dimensions and how no cell values are created when no point data is within their defined dimensions

This method was used on the whole glacier segment of the TLS and UAS data sets and then for just the face segment of the data sets. This separated the coverage percentages for the whole extent of the glacier and then for just the face or sloping portion. This allowed a way to compare how the collection types covered the whole glacier, both top and slope surface, and then how well the

methods perform on just a sloped surface removing any advantages in percentage that might have been gained on the more horizontal terrain.

Different resolutions were used in the rasterization process to change the dimensions of the cells to gather more understanding of the coverage as the density of the point clouds change throughout the study area in different ways depending on the collection type. With TLS the point density lessons with horizontal distance from the scanner. With the UAS data the point density decreases vertical at point when the ground is farther from the camera. The different resolution chosen were based on common Digital Elevation Model (DEM) and Digital Surface Model (DSM) resolutions used in studies. In one study, the DSMs generated from high-resolution imagery was from 10 cm to 1 meter (V. Yordanov et al, 2019). In Alexander's project DSMs with a GSD of 25 cm were produced. In another study, DSMs at 2.5 cm/pixel were created (M. Disney et al, 2019). Then with I. Colomina and P. Molina's (2014) project there were several cameras tested where the DSM came out to 5 cm/pixel (I. Colomina, 2014). The projects used cameras from 12 to 40 megapixels which appears to currently be the common drone pixel resolution. Pix4D has an option to create DSMs from the point cloud data which is typically 5 times the orthomosaic GSD. Considering this, the Rock Glacier DSM resolution from this projects data was 15 cm. The three resolutions chosen for the rasterization process based on this information were 0.5 cm, 0.15 cm, and 0.25 cm.

2.3.6 DEM Interpolations

Most UAS and laser scanning data is transformed into DEMs for 2.5D analysis for their ease of use, storage, and processing capabilities. Several types of common interpolation methods were used to transform the point cloud data. CloudCompare's rasterization tool was used once more with cells values being the average of those points falling within the cells and with missing cells being interpolated using linear nearest neighbor (CloudCompare, n.d.). There are no other interpolation options in CloudCompare so the other methods were implemented using ArcGIS Pro. Those methods were triangulation, linear, Inverse Distance Weighing (IDW), Nearest Neighbor (NN) and Simple. Averaging is a local method that does not interpolate and is non-smoothing in which intuitively the peaks and lows are under and overestimated (M. Rak et al, 2014). Natural neighbor is a local interpolation method with a smooth predictor (M. Rak et al, 2014). Inverse distance creates weights inversely proportional to the squared distances from the pixel and is considered to be a global interpolator with a smooth predictor (M. Rak et al, 2014). Figure 15

provides an example of how these methods can differ. In this study, the first name describes whether it is a Binning which bases raster values from point inside the defined grid or Triangulation method like a Triangular Irregular Network (TIN) with vertices to the point values. The second name describes the cell assignment used and the third name describes the methods used for filling the voidsd. These interpolated surfaces created from the point clouds were then used in a typical raster calculation for a change detection analysis to see how the results differ from that of the points clouds change analysis.
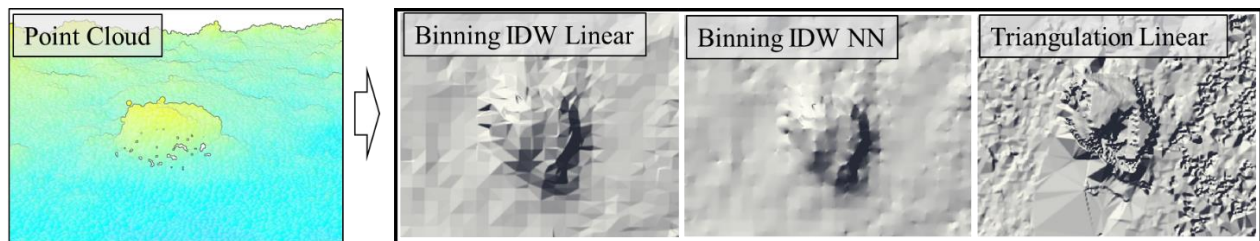
Figure 15 Provides an example of how point clouds and different interpolations can visually vary

The interpolations were performed with three different resolutions for the same reasons described in the rasterization process. The resolutions used were 5, 15, and 25 cm to be within similarity to popular DEM resolutions used.

2.3.7 DEM Change Detection: DoD

It is regular practice, when performing change analysis for glacier tracking, for the point clouds to be resampled and gridded into DEMs or DSMs. However, this will only allow elevation changes in the horizontal plane to be recognized (V. Yordanov, 2019). But the most common comparison of point clouds is done after they are transformed into DEMs (D. Lague, 2013). Performing a typical change detection between DEMs of comparison against the point cloud results was performed for this reason.

The change detection analysis between the produced DSM/DEM data from 2012 and 2019 was performed using a plugin within QGIS. The plugin is titled "Three-D Change Detection". This plugin was helpful in speeding up the calculations, applying symbology, and converting to hill shade for easier inspection. Each pair with the same interpolation methods and resolution was processed to create the resulting change values seen in the results.

2.3.8 Point Cloud Change Detection: M3C2

There are several point cloud change detection methods currently available and being used. Studies for surface change detection have use Cloud to Cloud (C2C), Cloud to Mesh (C2M), and Multiscale Model to Model Cloud Comparison (M3C2) distance calculations (D. Lague, 2013; T. Barnhart & T. Crosby, 2013; E. Bash & B. Moorman & A. Gunther, 2018; N. Ahmad Fuad et al, 2018; P. Rossi, 2017). C2C and C2M type comparisons are said to deliver good approximations of surface change but they do not consider the local orientation of surfaces portrayed by point clouds (T. Barnhart & B. Crosby, 2013). If the orientation is not considered it can cause the displacement calculated between the point clouds to be affected by point density, topographic shading and changes in surface roughness. A study comparing M3C2 and C2M found that, M3C2 provides a better accounting of sources for uncertainty (T. Barnhart, 2013).

To do the point cloud change detection, M32C was used as studies found that it provided the most realistic measurement of changes and could account for uncertainty (D. Lague, 2013). As opposed to DoD, this method accounts for localized surface roughness and slope that provides a more realistic surface change (S. Vivero, 2019). As can be seen in the figure below, user input for the diameter, D, is defined to determine the points used to calculate the normal direction of the terrain (Bash et al. 2018). Areas without point within the diameter are not calculated.
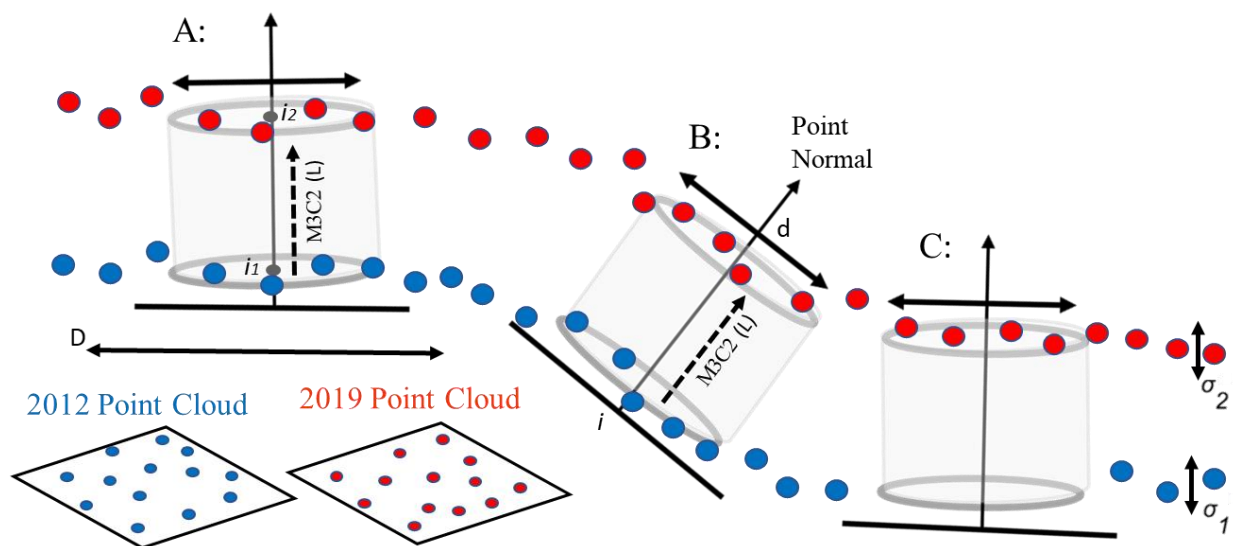
Figure 16 Illustration of the M3C2 algorithm process in selecting and calculating points. The normal direction to the 2019 UAS point cloud is computed based on a diameter, D. Projection of the cylinder, diameter d, along normal direction to calculate distance between the two point clouds. Local roughness, σd, can be higher in steep terrain, which influences the confidence value, C95%. (D. Lague, 2013; T. Barnhart & T. Crosby, 2013; E. Bash & B. Moorman & A. Gunther, 2018)

Being able to quantify a level of uncertainty of the measurements sets this method apart from most other surface change analyses. The confidence interval ($C_{95\%}$) is calculated based on the local roughness of each point cloud within the cylinder, points within the cylinder, and a registration error, Equation 1 (E. Bash, B. Moorman, A. Gunther, 2018).

$$C_{95\%}(P) = \pm 1.96 \left(\sqrt{\frac{\sigma_1(d)^2}{n_1} + \frac{\sigma_2(d)^2}{n_2}} + reg \right) \tag{1}$$

Equation 1 When the registration error is set by the user and related to instrument noise or mapping errors this equation could provide an estimate of confidence making it possible to quantify uncertainty which separates the method from most others (D. Lague, 2013)

For the change detections performed, the Gaussian statistical tool was used to determine the best fitting diameter for normal computing. The TLS was used as the reference from which the core points were defined.

4. Results and Discussion

This section reviews the results that the methods and data processing steps were leading up to. These topics include the comparison of the data collection completeness, point cloud and DEM accuracy, and M3C2 and DoD results. The data collection or acquisition methods are compared in the ability to provide consistent point density and continuity with less occlusions and increased perspectives. The point clouds of a feature in the model and various interpolated DEM versions of it are compared to see how the accuracies differ when examining the features height and area measurements. Then the results of the change analysis from the routine DoD and the M3C2 point cloud distances are compared to see the effects of the data transformations and change detection methods.

4.1. Data Acquisition Completeness

To develop an understanding of which current high-resolution and 3D collection methods potentially provide the best completeness, the UAS data collection with both nadir and terrain adjusted oblique imagery is compared to traditional UAS nadir imagery and TLS data collections in addition to the combination of UAS nadir and TLS that has been seen in recent studies. As mentioned earlier, the way in which point density or resolution across the study area differ depends

on the collection method used. The TLS scanner's, using active sensing with LiDAR from a horizontal fixed position, coverage and point density varies differently across the study area as compared to the UAS platform with a passive optical sensor. However, in both cases, simply the farther the sensor is the less quality or point density there will be without considering the effects of data occlusions from the viewing angle. In Figure 18 it can be seen how the point density varies along the surface of the glacier depending on the collection method. These differences exhibited will help explain some of the differences in completeness later in this section.

The point densities being represented in Figure 18 are based on the amount of points within a 25 cm radius of each point with green being 100 or more points and with red being 15 or below and with black equaling no points. The search radius chosen was based on common UAS high-resolution data sets providing a reference for expectations and seeing how much information is provided within 25 cm of each point.
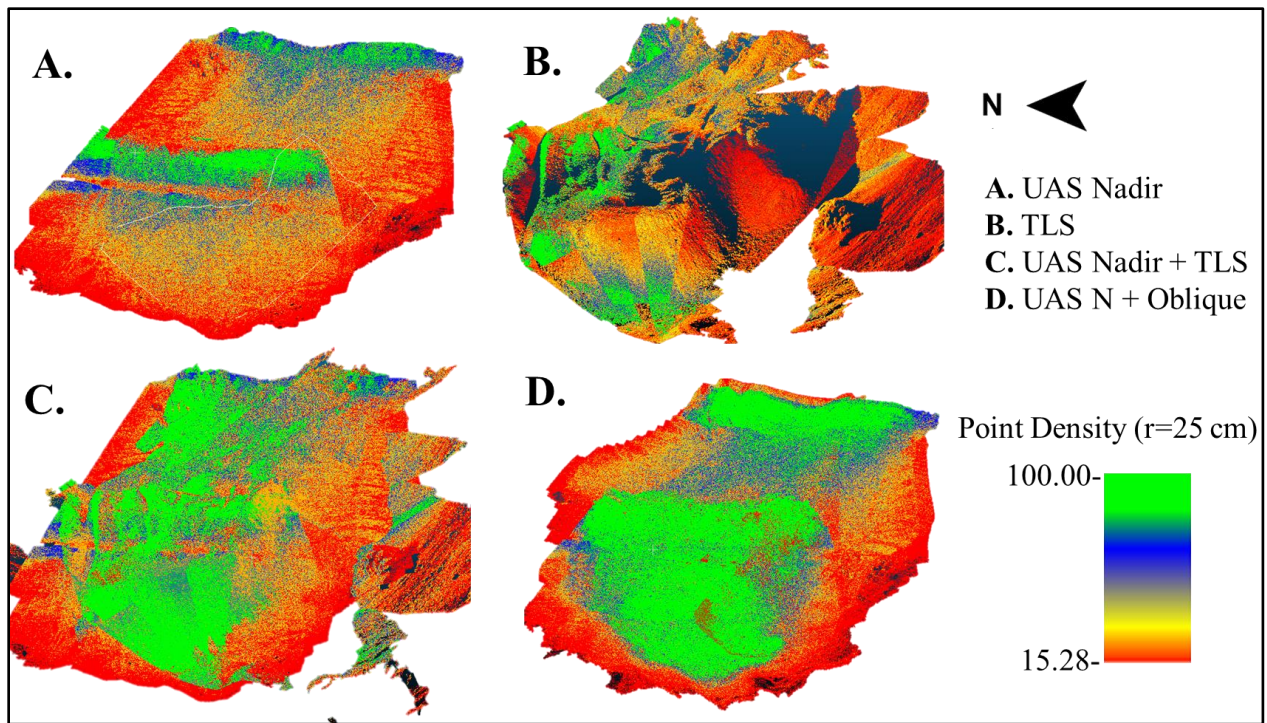
Figure 17 Point densities throughout the study area from each collection method is compared based on a defined radius around each point

As can be seen in Figure 18, TLS point density fades quickly from the sensor because of laser dispersion or points disappear completely with occluded areas from the complex topography of the rock glacier. These occlusions include areas on the side and tops of the glacier as its shape

changes drastically on all dimensional sides making it difficult to capture the full extent from the fixed perspective of a TLS. On the other hand, the UAS data is collected in a dynamic manner rather than a fixed position. When the sensor being able to move across the study area it is possible to get a more consistent collection. With the nadir UAS imagery and with the altitude being mostly uniform across the study area, the point density produced directly corresponds with the distance from the ground with extreme slopes also causing affects because of the viewing angle of the sensor to the ground regardless of its movement. The UAS flight height was different for the first day and front half of the glacier as compared to the third day and back half of the glacier to try and compensate for the steep altitude changes of the glacier surface. It can be seen, in Figure 18 (A), where the glacier surface was closest to the drone sensor on those two separate collections. Then in Figure 18 (C), the nadir UAS imagery and TLS data are combined which shows how they complement one another with added density around in area they were lacking. However, there are still portions of low density on south facing slopes of the glacier because of the TLS scan locations and the UAS camera viewing angle and distance. In Figure 18 (D), the oblique imagery with terrain height corrections at the front of the glacier shows the possible improvements in point density along with consistency and coverage. There is a lack of point density in the middle of the glacier due to no terrain height corrections in that portion although it is slightly increased as compared to the UAS nadir because of the 3D model flight characteristics such as the double gridded path and oblique imagery. In all cases it depends on where the sensor is placed and with the multirotor UAS it was possible to place the sensor evenly along the face of the glacier while also changing the camera angle. Taking advantage of these methods that are particular to multirotor UAS, the potential benefits can already begin to be seen.

Data gaps or occluded areas of the glacier are present and vary depending on the collection method's field of view (FOV). In Figure 19, a closer look is taken at some perceptual data depravations and gaps that exist from the different collection methods that were not mentioned in the previous paragraph.
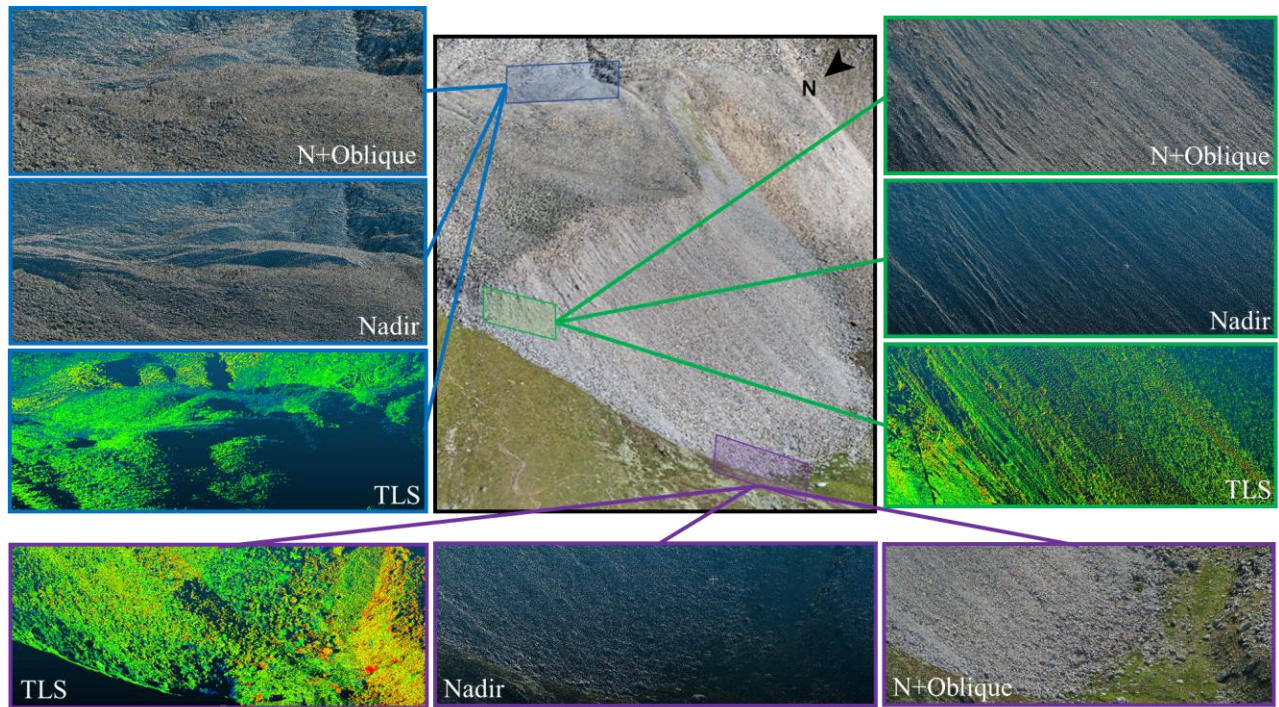
Figure 18 Comparison of the perceptual data gaps present on the glacier's surface depending on the collection method

Data gaps in the TLS data exist behind large boulders and rugged or pitted terrain on sides that are opposite to the sensor. In this case, there are occlusions on the east side of boulders and protrusions on the face of the glacier. Then there are occlusions present on the south facing sides of boulders and terrain on top of the glacier. The lack of scans from the south side of the glacier attribute to many of these occlusions. However, to gather scans on this side would have required dangerous traversing on the glacier surface and more collection days. The nadir only UAS model has severely degraded point density and gaps on the sides of highly sloped topography which is common on the top surface of this glacier. The nadir imagery also lacks views underneath boulders and protrusions on the glacier's face and around sides of features at the base. In addition, the point density is greatly reduced down the face and base of the glacier because of the progressively reduced scale from the UAS's sensor to the surface. The reduced point density worsens those data gaps present. Having oblique imagery from the UAS at all sides around the top surface and down the face of the glacier with height corrections for the slope, fills in the data voids present in nadir only while also adding higher and more consistent point density as can be seen in Figure 18.

As mentioned in the data processing section, different dimensional views of the 3D models, created from each collection method, was rasterized using various resolutions as explained in section 2.3.5.

The models were rasterized from the X dimension as the view from the front of the glacier and the Z dimension as the view above the glacier. The areas with no points within the defined raster cell dimension in would be given no values in that dimension. The amount of non-empty raster cells could be calculated providing a means of quantification of data coverage and density of the most important sides, front and top, of the 3D representation of the glacier. The values from each view were averaged together for each method to compare the total coverages three dimensionally. The results of the coverage of each method across the whole glacier with different grid sizes can be found in Figure 19.
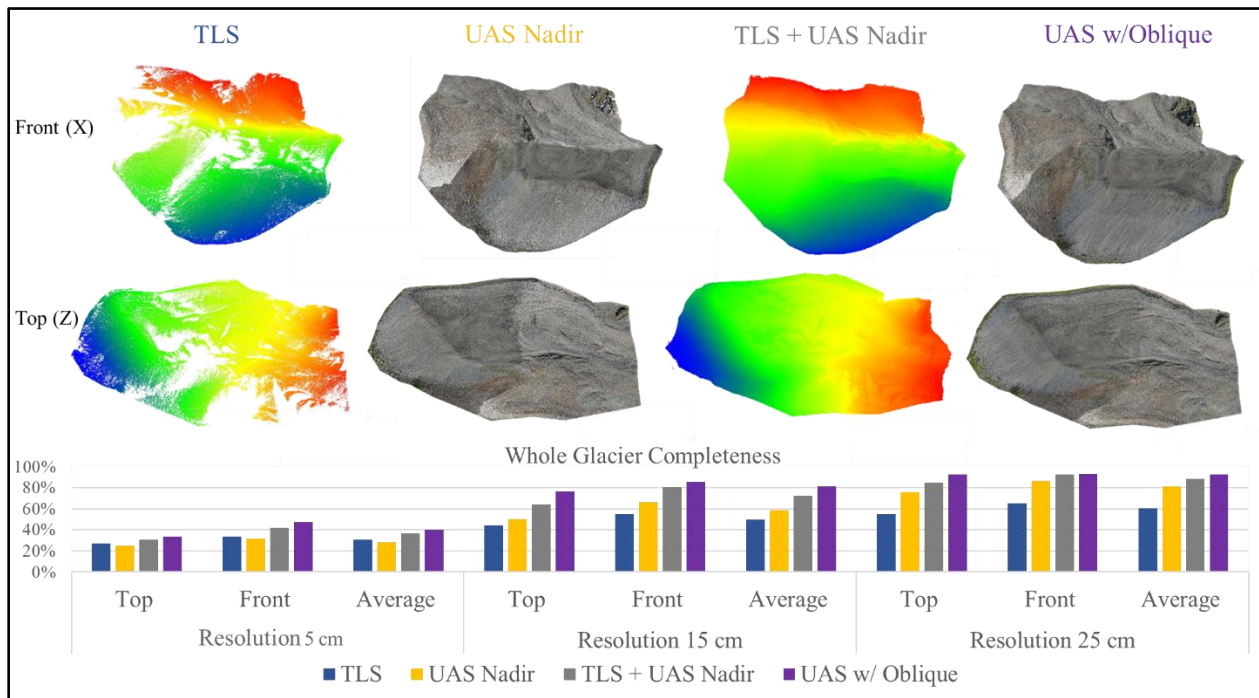
Figure 19. Results of the multidimensional rasterization of the 3D glacier models with percentage of non-empty cells to quantify the completeness of the collection method used

The images in Figure 19 are the resulting rasterizations at a resolution of 15 cm and they can be used to understand the view from the dimensions used and the obvious areas of data gaps from that perception. With the raster images it can be clearly seen that there are many areas of empty cells from both perspectives. In the nadir UAS raster images it can be seen that there is an increase of empty cells at the base of the face in both dimensions and then on the top surface in the X dimensions because of the sides of the of steep slopes of the rugged terrain. The TLS combined with UAS nadir data appears to complement and fill in where the two collections methods fall

short. The UAS nadir with oblique imagery appears to also be complete before considering the percentages.

Table 5 Completeness percentages of entire glacier depending on the perceptual view and separated by collection method and resolution of rasterization. The percentages are calculated by the amount of non-empty cells present depending on the intersection of point cloud values within the specified dimension of each cell or resolution as specified.

Rasterization completeness % (Whole Glacier)								
	Resolution 5 cm			Resolution 15 cm			Resolution 25 cm		
Acquisition Type	Top (z)	Front (x)	Average	Top (z)	Front (x)	Average	Top (z)	Front (x)	Average
TLS	27.32%	33.38%	30.35%	44.22%	54.96%	49.59%	55.04%	65.29%	60.17%
UAS Nadir	24.99%	32.08%	28.54%	50.41%	66.26%	58.34%	75.89%	86.39%	81.14%
TLS + UAS Nadir	30.39%	42.22%	36.31%	64.04%	80.58%	72.31%	85.00%	92.30%	88.65%
UAS w/ Oblique	33.54%	47.13%	40.34%	76.73%	85.66%	81.20%	92.49%	93.05%	92.77%

The resulting percentages, as expected, shows that the TLS's coverage is better in the X dimension as compared to its coverage in the Z. At 5cm resolution the TLS has better coverage with an average percentage greater by approximately 2% than the nadir UAS imagery which is most likely due to the point cloud density. The density around the base of the glacier, as seen earlier, is higher for the TLS because of its position during collection as compared to the UAS nadir flights. This is opposite at 15 cm and 25 cm resolution as the point density matters less because it is high enough for at least one point or more to be captured within those grid distances. Now the data gaps around the boulders and rugged terrain make greater impacts on the percentages with greater point distances than caused by decreased resolutions. The TLS data has more data occlusions than the UAS nadir data in both dimensions resulting in lower coverage with larger grids. The average coverage percentage of the Nadir UAS imagery is higher by approximately 8.5% with the 15 cm resolution and 21% in the 25 cm resolution. When the TLS and nadir UAS data are combined the percentages increase from the next best averages by 6% percent at 5 cm, 14% at 15 cm, and 7.5% at 25 cm resolutions. However, when the oblique imagery is added to the nadir imagery of the UAS collections the percentages in coverage increase beyond that of the TLS and UAS nadir combination. The UAS with oblique imagery increase the average coverage by 12.75% at 5cm, 9% at 15 cm, and 4% at 25 cm. The exact percentages can be seen in Table 5. The percentages are closer at the front (X) perspectives and only .75% different at 25 cm which can be attributed to the benefits of the TLS perspective. There are larger differences at the top (Z) perspectives which could be attributed to the UAS resolution consistency from terrain height corrections and lack of

occlusions from multidirectional oblique imagery. At all resolutions for analysis of the entire extent of the glacier the oblique imagery with terrain adjustment combined with the nadir imagery has the best completeness and coverage in both separate and combined dimensions.

The face of the glacier was segmented from the rest of the model to examine the completeness each method can provide on a steeply sloped surface. The results are particularly important to rock glacier studies as the face of the glacier is typically highly sloped, highly dynamic, and is key to several types of assessments. The results of the segmentation and rasterization can be seen in Figure 20.

Figure 20 Results of the multidimensional rasterization of the segmented face of the 3D glacier models with percentage of non-empty cells to quantify the completeness and effectiveness of collection methods on highly sloped surface
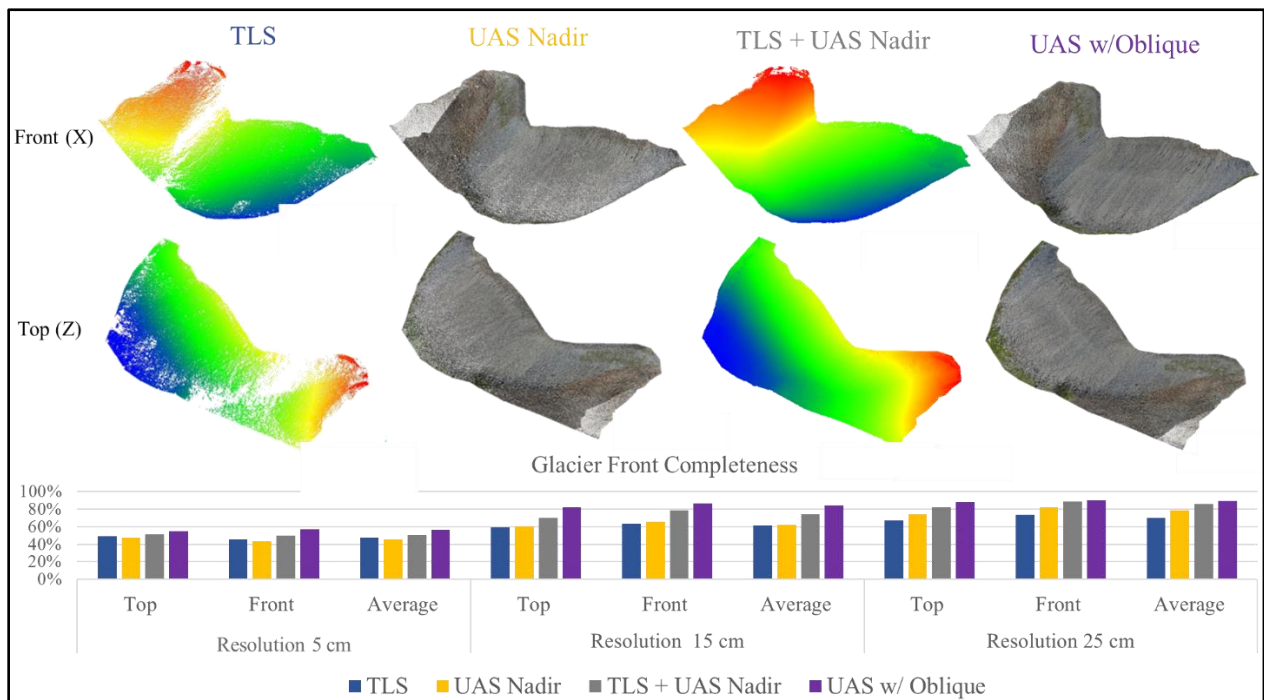
Table 6 Completeness Percentage for the glacier face depending on the perceptual view and separated by collection method and resolution of rasterization. The percentages are calculated by the amount of non-empty cells prevent depending on the intersection of point cloud values within the specified dimension of each cell or resolution as specified.

Rasterization completeness % (Glacier Front)								
	Resolution 5 cm			Resolution 15 cm			Resolution 25 cm		
Acquisition Type	Top (z)	Front (x)	Average	Top (z)	Front (x)	Average	Top (z)	Front (x)	Average
TLS	49.02%	45.65%	47.34%	59.13%	63.15%	61.14%	66.80%	73.35%	70.08%
UAS Nadir	47.92%	43.45%	45.69%	60.22%	65.38%	62.08%	74.35%	82.28%	78.32%
TLS + UAS Nadir	50.85%	49.78%	50.32%	69.70%	78.46%	74.08%	82.37%	88.78%	85.58%
UAS w/ Oblique	55.10%	57.17%	56.13%	82.06%	86.12%	84.09%	87.84%	89.97%	88.91%

The coverage results for the face of the glacier is similar to previous results with the whole extent of the glacier. However, the TLS data has more coverage from the top (Z) view at 5 cm resolution than its front (X) perspective this time. Once again, the TLS provides more coverage at 5 cm when the cell size is small enough for the point density to have the largest impact but then the UAS nadir provides more average coverage at 15 cm and 25 cm resolution. However, the average completeness percentages are closer this time. The TLS provides a better average coverage by 2% at 5 cm and then the UAS nadir provides better coverage by 1% at 15 cm and 8% percent at 25 cm. These percentages are improved upon when the TLS and UAS nadir are combined to provide an average increase of 5% at 5cm, 12% at 15 cm, and 7% at 25 cm. The oblique and nadir UAS imagery combination still outperforms with an average increase of 6% at 5 cm, 8% at 15 cm, and 3% at 25 cm. With the results in this section it makes it possible to develop an idea of the amount of information completeness that can be gathered with each collection method with UAS oblique imagery combined with nadir providing the most promise.

From the objectives it was first sought out to discover if multirotor UAS are capable of capturing data for point clouds with perspectives that would lessen the need for TLS considering that UAS nadir imagery is being combined with TLS as a recent method in studies to provide the most inclusive three-dimensional capture of rock glacier terrain (Fugazza et al. 2018; J. Šašak, 2019). The flight paths commonly seen with multirotor UAS to capture facets of houses in real estate was adopted for use in an attempt to capture the best three-dimensional data of rock glacier terrain (K. Mwangangi, 2019) The flight advantages were used to obtain oblique imagery that was corrected for height at the face of the glacier while combining it with nadir imagery and found that this technique can potentially provide more data completion than the use of TLS LiDAR and UAS nadir imagery used separately or combined. This method on average increases the completion of 3D collection by 8.6% as compared to the other methods from this study. The advantage of multirotor UAS as portrayed in Figure 1, is its ability to move the sensor in any direction which can be coined as a dynamic collection method as compared to the static position of a TLS scan.

Providing evidence that a UAS can deliver the most perspectives in data collection is logistically beneficial as systems are becoming more compact and cheaper (I. Colomina, 2014). The UAS used to collect the data in this project weighed at 0.9 g and could be packed in a 60cm x 30cm x 20cm case carried by one person as compared to the TLS weight over 13 kg which had to be carried by

at least two people. The cost of TLS scanner used was approximately 16000 euros while the cost of the UAS used was 1250 euros. It has been found in other studies that UAS collection is much cheaper than TLS as well (Vivero, S. 2019; Disney, M. 2019) In addition, With the progress in photogrammetry processing, the appeal of using UAS for data collection has been increasing and further benefiting the results of this study. Photogrammetry use has increased with the widespread use of UAS and has caused an up rise in processing abilities with many new competing software (I. Colomina, 2014). Using photogrammetry has surpassed LiDAR in popularity in creating point cloud data (Remondino et al., 2018). Because of this competing popularity, studies have tested the accuracy of photogrammetry derived point clouds and found that it is just as accurate as LiDAR (J. Ryan et al, 2015). This further illustrates the benefits of being able to solely use a UAS for complete perspective gains.

4.2. Point Cloud and DEM Accuracies

Much of the current practice for glacier monitoring is to transform LiDAR or photogrammetry point clouds into DEMs because of the readily known tools, storage, and perceived processing limitations (D. Fugazza, 2018; M. Disney,2019; W.W. Immerzeel, 2017; E. Schwalbe, 2008). This section compares the results of the transformations of the point clouds into DEMs from the TLS, UAS nadir, and TLS nadir + oblique data using different popular types of interpolations as discussed in the data processing sub section 2.3.6. The comparisons are made by measuring the area and height of a boulder at the base of the glacier face within the point clouds and DEMs to see the differences vertically (Z) and horizontally (X,Y) between the data types, transformations, and collection methods. All results are compared against measurements within Pix4D that are calibrated from ground truthing. The results intend to provide a better understanding of the effects of DEM transformations along with the accuracy of point clouds.

The GCPs used for the project were placed on boxes for 3D georeferencing. These boxes, with their known dimensions, were also able to be used as ground truthing mechanisms to test the accuracy of the photogrammetry process and measurements within pix4D. The location of the GCP box and boulder along with an illustration of the measurements made can be found in Figure 21.
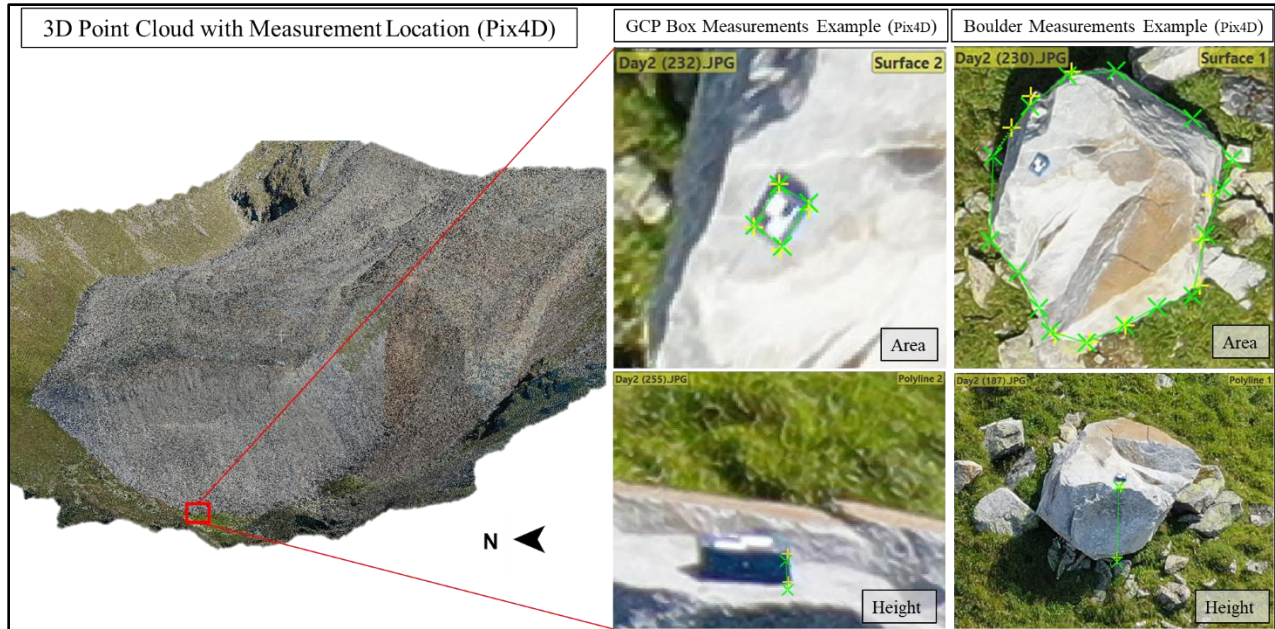
Figure 21 Illustrating the location of the boulder and its measurements, verified using 3D GCP known dimensions, that are used to check the point cloud and DEM accuracies of the same boulder

Table 7 Table (left) sowing the measurements done in pix4D of the GCP box and test boulder whith (right) ground truthing measurement of the GCP box to determine Pix4D measurement accuracy

Pix4D Measurements				GCP Box Ground Truth Measurements	
Measurement	GCP Box	Surface Boulder		Measurement	GCP Box (Actual)
Area (m^2)	.06 (+/- .05)	15.83		Area (m^2)	.062
Height (m)	.11 (+/- .21)	2.73		Height (m)	.11

The recorded measurements for the GCP box during collection in the field was 31cm x 20cm x 11cm with 11cm being the height. In the pix4D software and measuring from nadir images the box's height was correctly projected at 11cm with a suggested error of +-2cm. The top area of the box was also correct in the software with an area of .06m^2 with the actual being .062m^2. Using these measurements as confirmation of accuracy within that portion of the photogrammetric model, the boulder at the base on the glacier's face with the GCP box used for ground truthing was measured using the same process and images. It's vertical height from the ground and its top visible surface area were measured as seen in the Figure 21. The boulder measured at an area of 15.83 m^2 and with a height of 2.73 m.

Area and height measurements of the boulder were made in the point cloud and DEM data using ArcGIS Pro to compare against its known dimensions. Each collection method's point clouds and

DEMs were compared to examine any differences in accuracies and effects on interpolations. A depiction of how the measurements were conducted with the point clouds and DEMs can be seen in Figure 22.

Each point cloud and DEM were measured using the same method within an ArcGIS Pro local scene. The values from each measurement was organized into a chart based on collection and data type along with the resolution used in each DEM interpolation. The actual dimensions that were derived of the boulder are included in the chart to be used for comparison as can be seen in Figure 23. The precise numerical values of the measurements can be found in Table 8 in the Appendix.
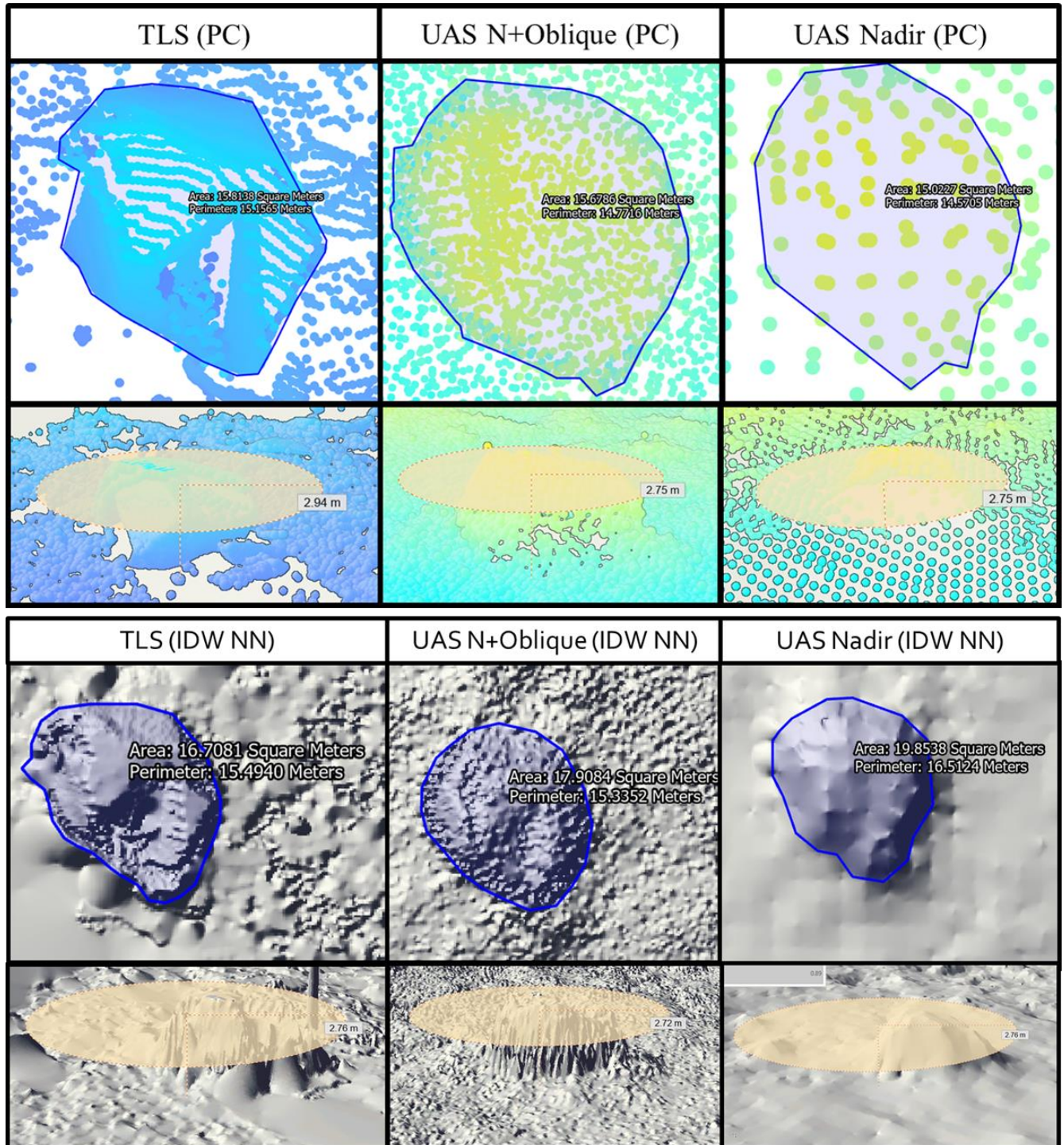
Figure 22 Depiction of how measurements were conducted in the ArcGIS Pro environment and examples of how the data sets differed depending on the collection method. Point cloud (PC) area and height measurements divided by collection type (top) and DEMs transformed from the point clouds using Inverse Distance Weighting (IDW) and Nearest Neighbor (NN) interpolations divided by collection methods (bottom).
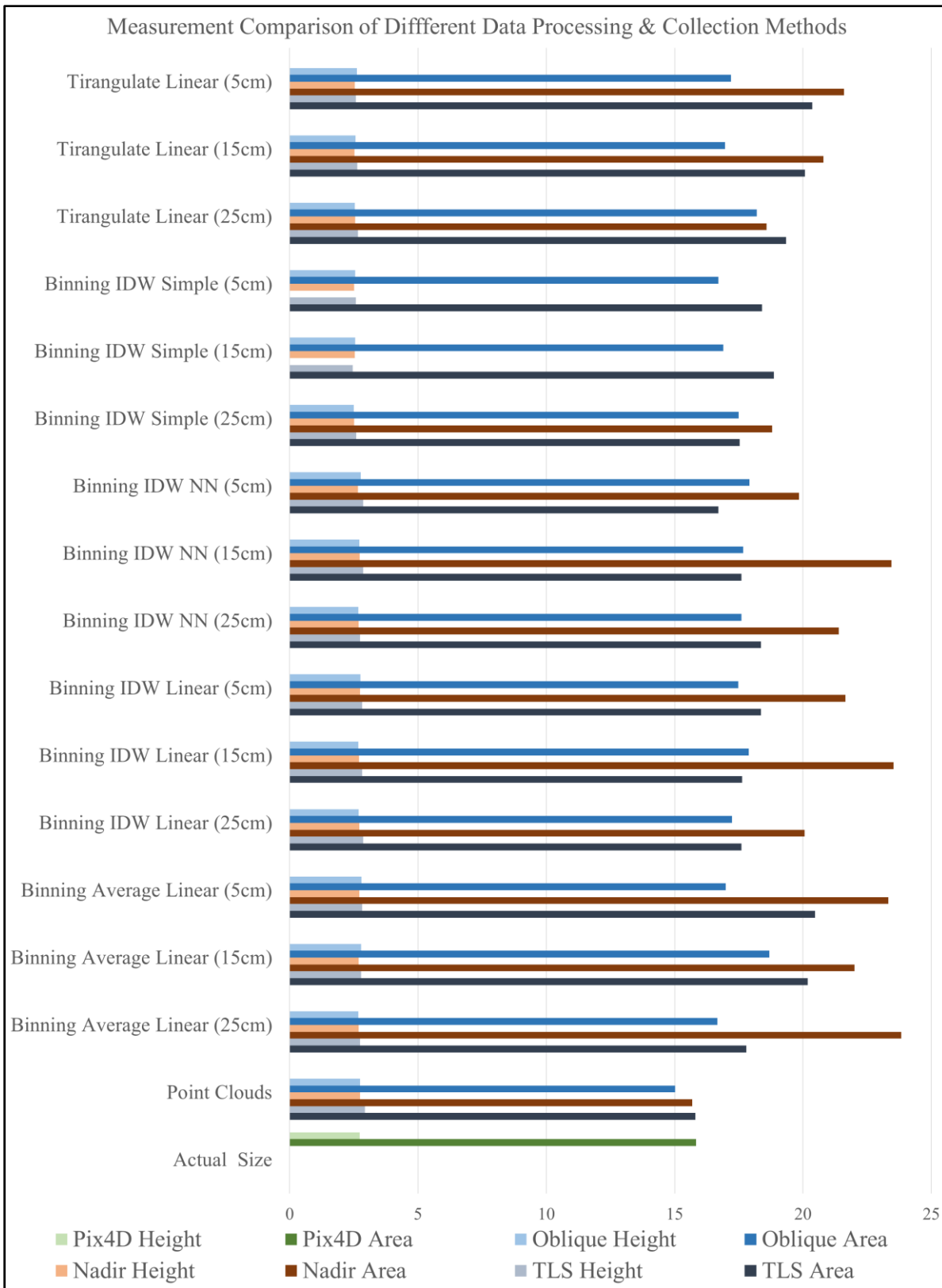
Figure 23 Comparison of the boulder area and height measurements of each DEM interpolation type at each common resolution against the point cloud and actual measurements.

It was found that the point cloud data is closest to the actual area and height values regardless of the collection method or point density. The average between the area measurements of the point clouds was 15.5 m providing an average of 0.33 m accuracy. The TLS point cloud had the highest accuracy with a measurement of 15.81m but had the least accurate height. The height measurement of the TLS method was 0.21m higher than the actual. The TLS inherently provides more accurate measurements horizontally than it does vertically because of the orientation of the sensor. The boulder was between two different scans so any errors in alignment could have also caused height inaccuracies.

When examining the DEM results, the height values remained relatively close to the actual height of the boulder. The average maximum height of the boulder among the DEM and collection methods was 2.67 m, an average accuracy of .06 m. However, the area of the boulder was far less precise in all DEM interpolation methods with the nadir UAS data resulting in the worst accuracy. The average area measurements within the DEMs with the different resolutions for each collection method was 18.6 m^2 for the TLS, 21.5 m^2 for the UAS nadir, and 17.44 m^2 for the UAS nadir + oblique as compared to the 15.83 m ^2 top surface area of the boulder in reality. Irrespective of the type, setting and resolution, DEM interpolation data no matter the type, setting, and resolution always gave a larger area than what it was in reality. This shows that DEM's maximum heights (Z) of a glacier surface boulder can be acceptable but the area or horizontal dimensions (X,Y) in which these heights exist are greatly fluctuated and exaggerated around the boulder.
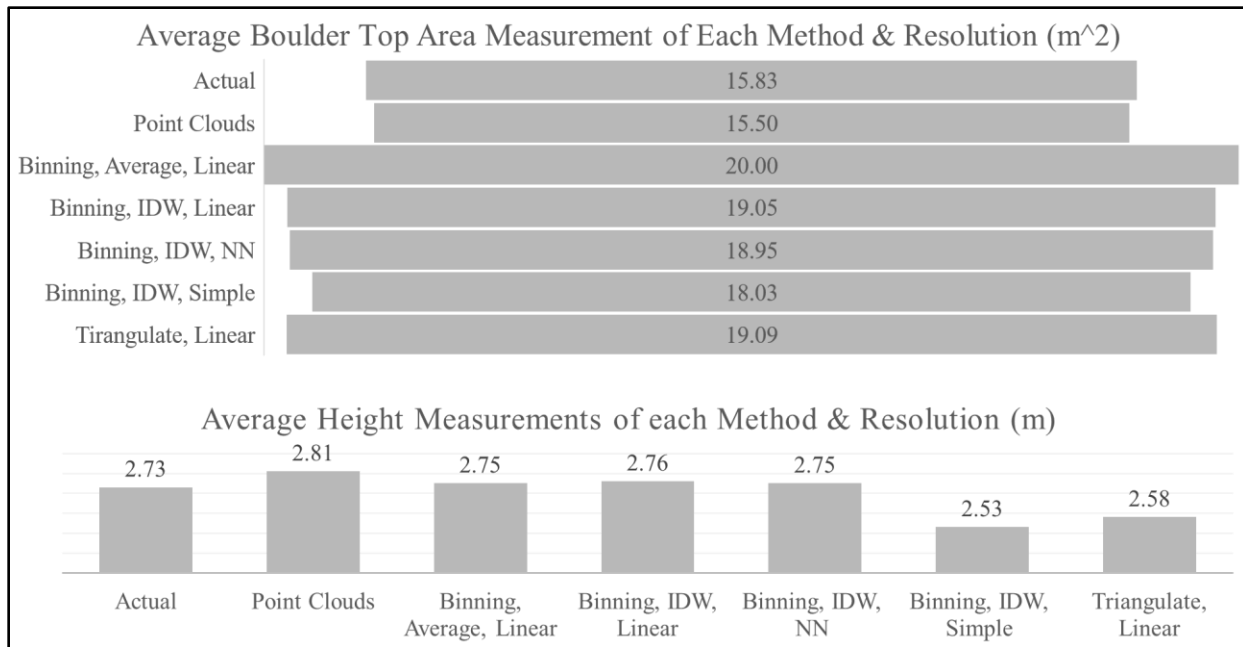
Figure 24 Providing the averages of measurement made per method with (top) showing the area measurements and (bottom) the height measurements made as compared to the actual values

Differences in results exist between each interpolation method and resolution. Majority of the time the higher resolutions provided better accuracies. However, it depends on the point density and data completeness. There are times that higher resolution does not mean better accuracy as seen with Triangulated Linear interpolation method and from the UAS nadir data. The 15 cm resolution for most methods used with the UAS nadir data gave higher inaccuracies in boulder area. With less density or missing data at higher resolution this means there will be more cells being interpolated without nearby values causing adverse effects in accuracy. Determining the resolution needed for best DEM accuracies when transforming from point cloud data can be tricky and can depend on point cloud density (D. Lague et al, 2013). Those methods that included the Simple interpolation method for interpolating the missing values were higher in accuracy because this method left large areas of missing values empty. However, this method still does not provide the horizontal accuracies of point cloud data.

These results show that DEM interpolation cause increased heights around surface items. Although the item's maximum height was correct the surface heights around the item became exaggerated and inaccurate because of the interpolation. It is particularly important to be aware of this with rock glaciers considering the entire surface is composed of similar boulders.

The second objective of this project was to discover how accurately the traditional use of DEMs captured the reality of the surface terrain of a rock glacier as compared to point cloud data. Rock glaciers are covered with rock debris that tumble and get displaced as the glacier creeps down slope with gravity. Because of this complex surface, maintaining the detail provided from data collection is important in providing a true understanding of displacement and movement. When comparing the accuracy of the point cloud data with the DEM interpolation methods, they both gave acceptable maximum heights of a boulder on the glacier surface but the point cloud on average gave better accuracies horizontally in the X and Y dimensions. When testing the top surface area of the boulder the point clouds provided an accuracy approximately 3 m^2 better than any of the DEM interpolation methods. This likely means that many of the other boulders on the glacier surface are most likely exaggerated in size and causing inflation in surrounding surface heights. This horizonal inflation can cause drastic effects on sloped areas because of the height values of the upper surface elements protruding horizontally into what should be the values of the lower sloped area. Which is supported in K. Stereńczak's (2017) study that found that the error of Digital Terrain Models (DTM), a type of DEM, increases with slope. Since some of the most important measurement of activity is at the highly sloped face of the glacier, this can be problematic.

4.3. Change Analysis Results Comparison

Change analysis was performed using point clouds with Multiscale Model to Model Cloud Comparison (M3C2) and common Difference of DEMs (DoD) methods as set up in the Data Processing subsections 2.3.7 and 2.6.8.The results of the methods are compared to reveal the differences that could exist between them. In addition, the results of different DoDs using various interpolation techniques for the DEMs (2.3.6) are used to examine their possible influence on the change detection process. Considerations from discoveries made in section 4.2 with DEM accuracies are meant to be used in correspondence with the DoD results for deriving conclusions.

The results of the M3C2 change analysis with the original point densities is visualized in Figure 25. The most recent point cloud surface has the new values projected on to it. The projection of values is based on the points from the reference surface which is the TLS 2012 data in this case. Because of the missing data from the 2012 TLS scan, the distances are only calculated from those points in the reference surface which is the TLS 2012 data in this case. It can be seen where there

are missing values because of the occluded areas in the TLS data. These values are not calculated to preserve accuracy. Those areas in yellow to red have proceeded forward or up from the past surface and those areas from blue to purple have receded back or down. Those areas closer to the neutral tan colors represent no movement.
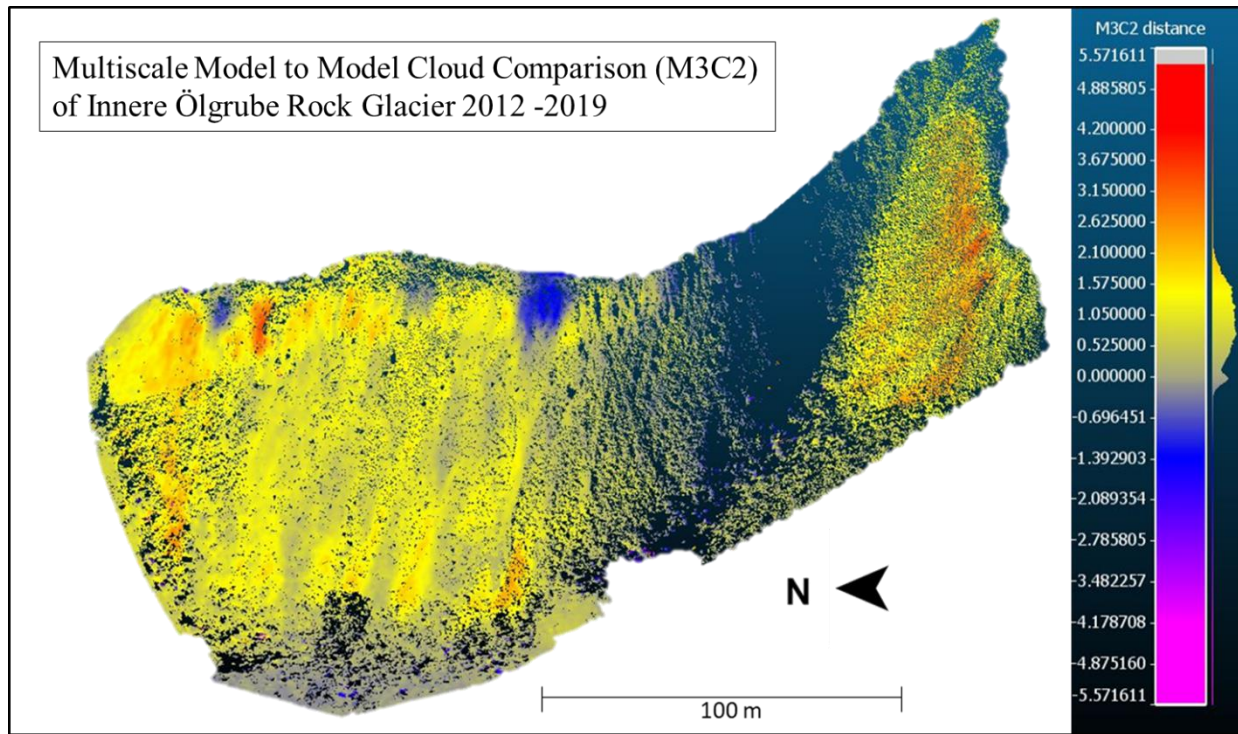
Figure 25. Visualization of results from the M3C2 algorithm to calculate change distances of the 2019 point cloud surface from the 2012 point cloud reference surface

An example of one of the DoD calculations can be seen in Figure 26 to be used in comparison with the previous M3C2 change visualization. The following example was from DEMs processed from the 2012 TLS and 2019 UAS nadir + oblique point cloud data transformed using Binning, Near, Linear interpolations at a 15 cm resolution. Those areas in red, yellow, dark green have increased in height from the 2012 TLS surface cell values to the 2019 UAS surface cell values with areas in blue and purple being a decrease. Those areas in light blue to light green have little to no change in values. In a visual comparison the results appear to be the same with some slight differences. However, those areas that were not calculated in the M3C2 results are being estimated based on interpolated surfaces. Furthermore, the areas of change appear larger and more distinctive than in M3C2. These considerations can be retained when examining the statistical values and histograms of the change values of both methods.
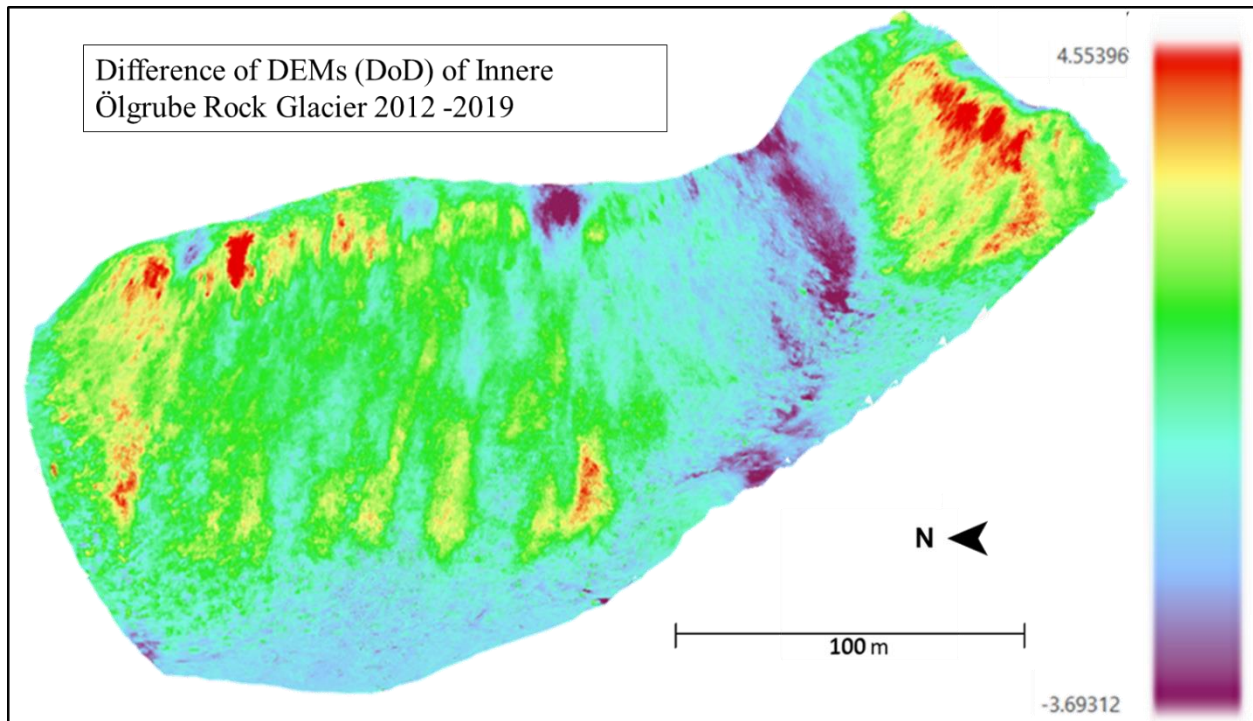
Figure 26 Difference of DEMs (DoD) visualization of results between the 2012 TLS and 2019 UAS nadir + oblique point cloud data that was interpolated using blank at blank resolution

All statistical results of the change analysis performed were organized into a bar chart which can be found in Figure 27 in order to compare how the change results differ using DEM data interpolated with different methods and how they compare to the M3C2 point cloud change results. The chart can be used to compare how the different methods effect the maximum increases and decrease of values and the common amounts of change with the standard deviation and mean values. Table 11 can be found in the Appendix with the statistical values used for the box chart. The histograms provide visualization and more detail into the distribution of the change values between methods and can be found in the Appendix in Figure 29.
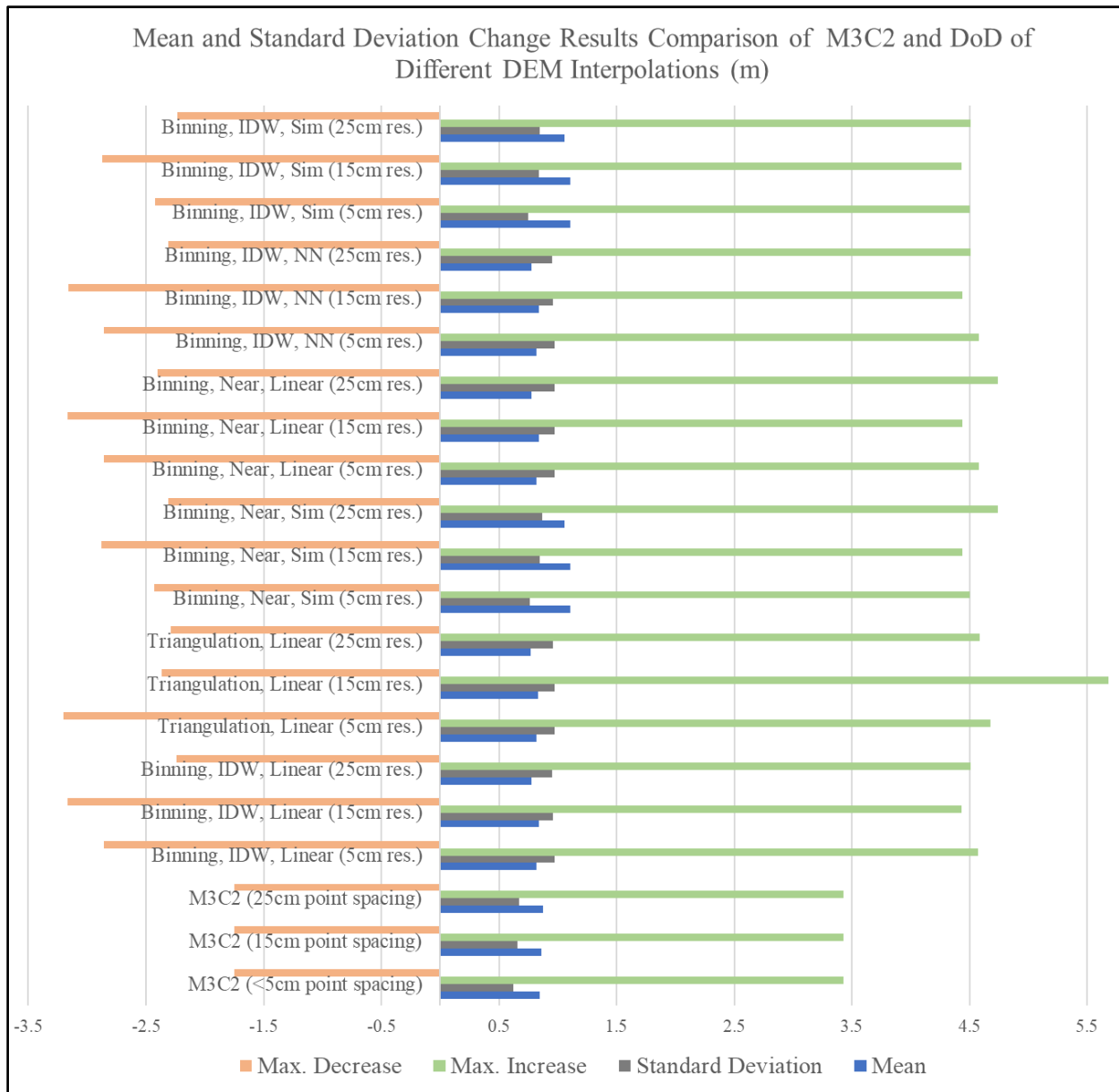
Figure 27 Bar graph for comparing the statistical results of each change analysis performed. The maximum increase, decrease/minimum, standard deviation, and mean of change of each method is represented in order to see how results are impacted based on method, resolution, and DEM interpolation used.

M3C2 change method was performed with three different point densities to mimic and to be compared to resolutions used for the DoD to see if any similarities in traits occur in resolution changes. The M3C2 original point densities were used for the first M3C2 results, then the TLS and UAS point clouds were resampled to 15 cm and 25 cm between each point before performing the next change analyses. The point density changes have little effect as the max and min values

of the analysis do not change but the standard deviation and mean do begin to gradually increase with the decreased point densities.

When comparing the M3C2 to DoD results, the max increases and decreases of M3C2 are lower than all of the DoD versions. The DoD maximum increase is always at least 1 m greater and the maximum decrease is always at least 0.48 meters greater than the M3C2 versions. The standard deviation of the M3C2 is less compared to all of the DoD's while the mean values are similar in many cases. The greatest difference in mean values is when the Simple interpolation is used which is the method that leaves cells empty in data gaps. The mean is 1.1 m for Binning, IDW, Simple and Binning, Near, Simple at every resolution as compared to approximate mean of .85 m of M3C2. However, with those methods using Simple interpolations the standard deviation is closest compared to other methods especially at the highest resolution. The DoD results are much more influenced by resolution of the data and provides a host of different results.

Among the DoD results, they differ depending on the interpolation method and resolution used. The max decrease is greater at 25 cm and less at 5 cm resolutions just showing the amount of change that can happen depending on the size of the cell and what point values are being considered for calculation of each cell value. The Triangulation Linear method results in a low mean at 25 cm and much higher mean at 15 cm resolution which shows better resolution does not always mean more precision because of the data gaps in the data. The smaller the cell or grid the more cells with no nearby values will need to be used to fill these voids. The resolution changes appear to have a greater influence on the mean as compare to the standard deviation except for the when the Simple method is used in which the opposite occurs.

The DoD results show that when interpolations are used for missing values the range in standard deviation is larger further exceeding those from M3C2. This suggests, along with what was seen in the previous section, that the interpolations expand the impacts that elevated features create on the local area around them. These elevated surfaces around features is what is often referred to as the smoothing effect and is the subtle transition from one interpolated cell to the next decreasing rigid changes in the surface which is in complete contrast to point clouds. The standard deviation becomes comparable to the point cloud data when the DEM has been processed without interpolating the missing values, using the Simple method, further concreting this thought. These affects are worse with less density as previously seen with the nadir imagery. With the TLS data

from 2012 it can be seen that missing data behind the rocks gets filled in with exaggerated height values and in the case seen in Figure 28, two rocks join together that would in turn create a larger area of change from the items movement from 2012 to 2019.
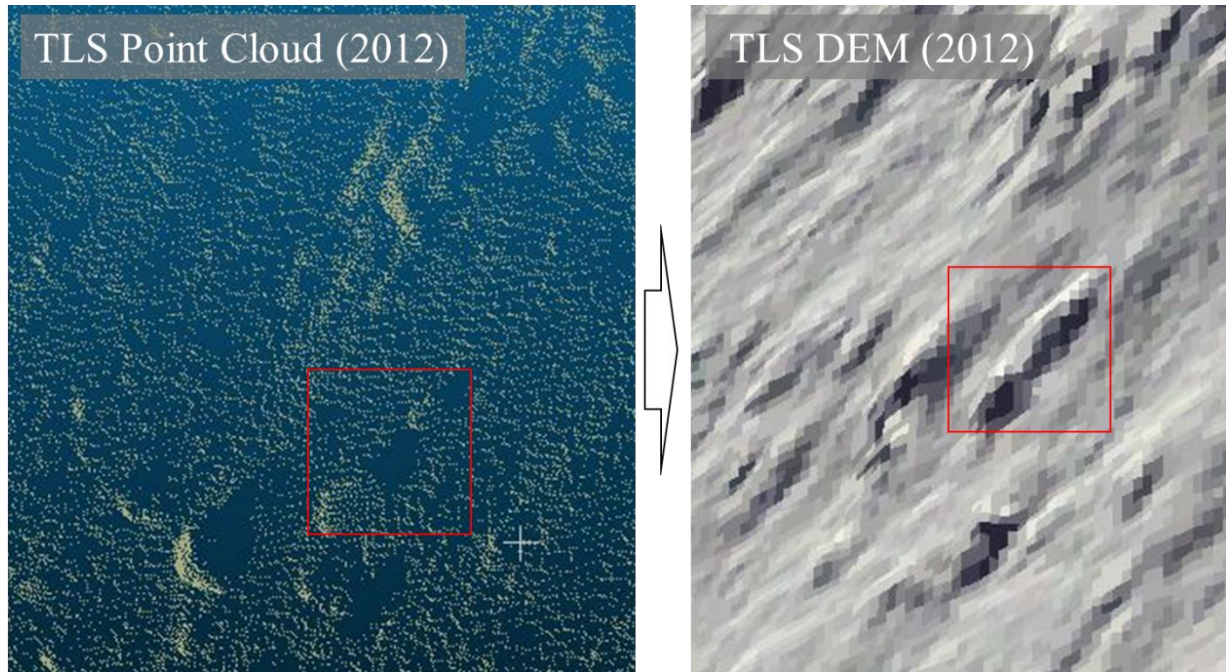
Figure 28 Point cloud data from the 2012 TLS scan (left) showing how areas of missing data is filled in with interpolations during the transformation to a DEM (right) causing inaccuracies in the size of surface features and exaggerations in surrounding heights.

The exaggerated size of surface items may also cause further increased inaccuracies because of the way change is measured with DoD. The DoD method calculates changes based on the height values between the corresponding cells at the same (X,Y) coordinates, pixel-to-pixel, of the two DEMs meaning that it only calculates changes in the z axis (D. Lague et al, 2013). With the expansion in sizes of surface items horizontally (X,Y) in DEM and causing the height of the surrounding area to increase, this would further heighten the area of the under sloping area. The effects of this would increase with the steepness in slope. This could be supported with D. Lague (2013) as he explains in his research that with the increase in steepness the amount of information from the DEM proportional decreases and with the interpolations introducing uncertainties for the cell elevation values. The expansion of the interpolated surface items on the upper parts of the slope would appear to greatly influence how the down sloping surface is being excluded or exaggerated. When DoD is being calculated, error would be further propagated because the Z distance will be greater having to measure from the past surface to exaggerated height of the upper

slope that has been caused by the interpolation and exaggeration of the surface item. In addition, the surface items present in the 2012 data will not be present in 2019 data and vice versa of the highly dynamic rock glacier creating even further errors on the change surface from movement of exaggerated masses.

One of the last focuses from the objectives in this project was to examine how Difference of DEMs (DoD) for change analysis behaves as compared to the newer point cloud method with M3C2. When calculating change between DEMs, the error present of from the interpolations as discussed in section 4.2 could be further propagated depending on the past surface and will cause inaccuracies in detecting height change and calculations for forward movement. This could also provide some reasoning to why DoD consistently, no matter the resolution or interpolation method used for deriving the DEM, always gave larger maximum and standard deviation values. In addition to this, the results showed the variability of DoD and the complexity of using DEMs as compared to M3C2 with point cloud data. The variability further complicates the situation as found in supporting studies that DoD error is very difficult or impossible to quantify (D. Lague,2013). The M3C2 results are far less affected by resolution because of the use of point cloud data which was proven to be much more accurate and better at conserving the true shape of surface items.

5. Conclusion & Final Remarks

5.1. Findings

This work presents elements for improving analysis of rock glaciers with the examination of newer 3D data capture and analysis methods. It was shown that multirotor UAS have the capability to capture angles similar to TLS but with better mobility and overall coverage. Integrating oblique imagery from the UAS provided an average of 8.6% more completeness in data for the entire glacier surface than traditional nadir UAS imagery and TLS methods whether combined or used separately. Because of this improved completeness, it showed that DEM detail and accuracy was benefited as compared to the other methods. However, point cloud data proved to create the most detailed and accurate representation of reality. DEM interpolations create inaccuracies in the size of surface elements and causing exaggerations in the surrounding surface heights. One of the many boulders on the rock glacier's surface had its dimensions tested for accuracy in the data sets where it was found that the average among the DEM interpolations provided an area of 19.02 m^2 for

the boulder and the point cloud provided 15.50 m^2 where the boulder is 15.83 m^2 in reality. These inaccuracies most likely affected the results of the Difference of DEMs (DoD) method as it provided at least a maximum increase on the surface by 1.1 m and decrease .85 m greater than the M3C2 method for DEM interpolations used. However, the use of different DEM resolutions and interpolation methods varied the statistical outputs of the DoD results showing the variability and uncertainties of this method. This study showed multirotor UAS can deliver completeness that can outperform recent 3D collection methods while using point cloud processing to benefit the data collection by maintaining the truest form of the glacier surface while having the ability to be processed with newer methods such as M3C2 which provides more consistent measurements that are in relation to the surface orientation.

5.2. Limitations

There were and could be limiting factors within this project's methodology. These limiting factors include the data gaps present in the 2012 TLS data, the increased RMSE with incorporation of oblique imagery, and then legal regulations on the flight of UASs for other studies wanting to repeat the presented methods. Data gaps from the 2012 TLS collection lessened the amount of surface change that could be calculated for the M3C2 methods. Having a more completed surface from the TLS data could have provided a more complete comparison of M3C2 and DoD. However, this reiterates the importance of data completion and the project was able to prove the negative effects of interpolations especially on larger data gaps.

The RMSE of the completely nadir imagery was 1.02 m then increased to 1.8 m when the oblique imagery was integrated into the processing. This was due to the complexity of angles and altitudes the UAS sensor was at when capturing the data causing increased local inaccuracies of the point cloud but most likely could be improved with MTPs. The original processed point cloud RMSE was much higher but improved with MTPs suggesting additional placement of MTPs could be tested for further improving the RMSE.

Legal restrictions on the flight of UAS platforms is a limiting factor for their use as compared to TLS systems. Every government has its own restrictions on operator licensing, operating times, operational flight parameters (altitude, distance, zones), and aircraft registration requirements. In some cases, this could require increased planning time and reduce the frequency at which data can be collected with UAS.

5.3. Future Work

This study used a multirotor UAS for both nadir and oblique image collection. Fixed-wing aircraft are commonly used because of their better flight endurance and being able to map large areas more efficiently. Future work could look at the use of integrating the combination of using a fixed-wing UAS to gather nadir imagery with a multirotor UAS to capture the oblique imagery. This could use the benefits of each systems with fixed-wing using its efficiency to cover more area and the multirotor UAS to gain better perspectives of details missed on the sides of terrain. The exact flight paths, procedures, and sensors to best complement one another would have to be further researched.

5.4. Conclusion

This study can be used by those in glacier geomorphology and similar disciplines to understand the benefits of detailed point cloud processing and potential in increased data coverages with multirotor UAS collection methods. As temperatures continue to increase and glaciers continue to decline at quicker rates, increased perspective and accuracy gains will provide improved predictions and assessments. This study shows that multirotor UAS have the potential to gather data from any of the angles captured from the other methods. Point cloud processing and analysis is becoming more popular as processing abilities improve with photogrammetry and the availability of UAS technologies. Multirotor UAS are progressively getting smaller, more reliable, and cheaper making their use more feasible and have the potential to become a singular unit for on demand, close proximity remote sensing needs while point cloud data can provide the truest forms of these increased details.

References

Abermann, J., Fischer, A., Lambrecht, A., & Geist, T. (2011). Glaciers in Ausrtia Past and Present. *The Cryosphere*.

Ahmad Fuad, N., Yusoff, A. ., Ismail, Z., & Majid, Z. (2018). Comparing The Performance of Point Cloud Registration Methods for Landslide Monitoring Using Mobile Laser Scanning Data, *XLII*(September), 3–5.

Barnhart, T. B., & Crosby, B. T. (2013). Comparing Two Methods of Surface Change Detection on an. *Remote Sensing*, 2813–2837. https://doi.org/10.3390/rs5062813

Bash, E. A., Moorman, B. J., & Gunther, A. (2018). Detecting Short-Term Surface Melt on an Arctic Glacier Using UAV Surveys. *Remote Sensing*. https://doi.org/10.3390/rs10101547

Bauer, A., & Paar, G. (2003). Terrestrial laser scanning for rock glacier monitoring, 1–6.

Buttschardt, T., & Malkus, A. (n.d.). Studienprojekt : „ Blockgletscher - Ölgrube " Kartierung des größten Blockgletschers der Ostalpen. *[Unpublished]*.

CloudCompare. (n.d.). CloudCompare User Manual.

Colomina, I., & Molina, P. (2014). ISPRS Journal of Photogrammetry and Remote Sensing Unmanned aerial systems for photogrammetry and remote sensing : A review. *ISPRS Journal of Photogrammetry and Remote Sensing*, *92*, 79–97. https://doi.org/10.1016/j.isprsjprs.2014.02.013

Czempinski, J., & Dabski, M. (2017). Lichenometry and Schmidt hammer tests in the Kaunertal glacier foreland (Ötztal Alps) during the AMADEE-15 Mars Mission Simulation. *Miscellanea Geographica*, *21*(4), 190–196. https://doi.org/10.1515/mgrsd-2017-0027

Disney, M., Burt, A., Calders, K., Schaaf, C., & Stovall, A. (2019). Innovations in Ground and Airborne Technologies as Reference and for Training and Validation : Terrestrial Laser Scanning (TLS). *Surveys in Geophysics*, *40*(4), 937–958. https://doi.org/10.1007/s10712-019-09527-x

Fugazza, D., Scaioni, M., Corti, M., Agata, C. D., Azzoni, R. S., Cernuschi, M., … Diolaiuti, G. A. (2018). Combination of UAV and terrestrial photogrammetry to assess rapid glacier evolution and map glacier hazards. *Natural Hazards and Earth System Sciences*, 1055–1071.

Groh, T., & Blöthe, J. H. (2019). Rock Glacier Kinematics in the Kaunertal , Ötztal. *Geosciences*, (2019).

Groos, A. R., Bertschinger, T. J., Kummer, C. M., Erlwein, S., Munz, L., & Philipp, A. (2019). The Potential of Low-Cost UAVs and Open-Source Photogrammetry Software for High-

Resolution Monitoring of Alpine Glaciers : A Case Study from the Kanderfirn (Swiss Alps). *Geosciences*.

Hanzer, F., Förster, K., Nemec, J., & Strasser, U. (2018). Projected cryospheric and hydrological impacts of 21st century climate change in the Ötztal Alps (Austria) simulated using a physically based approach. *Hydrology and Earth System Sciences*, 1593–1614.

Immerzeel, W. W., Kraaijenbrink, P. D. A., & Andreassen, L. M. (2017). Use of an Unmanned Aerial Vehicle to assess recent surface elevation change of Storbreen in. *The Cryosphere*. https://doi.org/10.5194/tc-2016-292

Kaufmann, V., Seier, G., Sulzer, W., Wecht, M., Liu, Q., Lauk, G., & Maurer, M. (2018). Rock Glacier Monitoring Using Aerial Photographs: Conventional vs. UAV-Based Mapping -A Comparative Study. *ISPRS*, *XLII*(October), 10–12.

Krainer, K., & He, X. (2006). Flow velocities of active rock glaciers in the Austrian alps Flow Velocities of Active Rock Glaciers in the Austrian. *Taylor & Francis*. https://doi.org/10.1111/j.0435-3676.2006.00300.x

Krainer, K., Kellerer-pirklbauer, A., Kaufmann, V., Lieb, G. K., Schrott, L., & Hausmann, H. (2012). Permafrost Research in Austria : History and recent advances. *Aurtrian Journal of Earth Sciences*, *105/2*, 2–11.

Lague, D., Brodu, N., Leroux, J., Rennes, G., Rennes, U., & Beaulieu, C. De. (n.d.). Accurate 3D comparison of complex topography with terrestrial laser scanner : application to the Rangitikei canyon (N-Z), (February 2013), 1–28.

Milner, A. M., Khamis, K., Battin, T. J., Brittain, J. E., Barrand, N. E., & Olafsson, S. (2017). Glacier shrinkage driving global changes in downstream systems. *PNAS*, 1–9. https://doi.org/10.1073/pnas.1619807114

Mwangangi, K. K. (2019). 3D building modelling using dense point clouds from UAV 3D building modelling using dense point clouds from UAV, (March).

Nesbit, P. R., & Hugenholtz, C. H. (2019). Enhancing UAV – SfM 3D Model Accuracy in High-Relief Landscapes by Incorporating Oblique Images. *Remote Sensing*, 1–24. https://doi.org/10.3390/rs11030239

Pepe, M., Fregonese, L., Scaioni, M., & Pepe, M. (2018). Planning airborne photogrammetry and remote- sensing missions with modern platforms and sensors. *European Journal of Remote Sensing*, *51*(1), 412–436. https://doi.org/10.1080/22797254.2018.1444945

Pix4D. (n.d.). Pix4Dmapper 4.1 User Manual.

Rak, M., Mayer, R., & Wozniak, A. (2014). Review of Interpolation Methods for Point Cloud Modelling In Coordinate Metrology, (April). https://doi.org/10.13140/2.1.2378.0485

Remondino, F., Toschi, I., Menna, F., Oezdemir, E., Morabito, D., Farella, E., & Nocerino, E. (2018). Point Cloud Acquisition *& amp; Structuring with contributions from FBK-3DOM members*. Trento. Retrieved from http://3dom.fbk.eu

Rossi, P., Dubbini, M., Mancini, F., & Mazzone, F. (2017). Combining nadir and oblique UAV imagery to reconstruct quarry topography : methodology and feasibility analysis Combining nadir and oblique UAV imagery to reconstruct quarry topography : methodology and feasibility analysis. *European Journal of Remote Sensing*, (April). https://doi.org/10.1080/22797254.2017.1313097

Ryan, J. C., Hubbard, A. L., Box, J. E., Todd, J., Christoffersen, P., Carr, J. R., … Snooke, N. (2015). UAV photogrammetry and structure from motion to assess calving dynamics at Store Glacier , a large outlet draining the Greenland ice sheet. *The Cryosphere*, 1–11. https://doi.org/10.5194/tc-9-1-2015

Šašak, J., Gallay, M., Kanuk, J., Hofierka, J., & Minar, J. (2019). Combined Use of Terrestrial Laser Scanning and UAV Photogrammetry in Mapping Alpine Terrain. *Remote Sensing*.

Schwalbe, E., Maas, H., & Ewert, H. (2008). Glacier velocity determination from multi temporal terrestrial long-range laser scanner point clouds Glacier Velocity Determination From Multi Temporal Terrestrial Long Range Laser Scanner point Clouds, (January).

Sommaruga, R. (2015). When glaciers and ice sheets melt : consequences for planktonic organisms. *Journal of Plankton Research*, *37*, 509–518. https://doi.org/10.1093/plankt/fbv027

Stereńczak, K., Ciesielski, M., Balazy, R., & Zawiła-, T. (2017). Comparison of various algorithms for DTM interpolation from LIDAR data in dense mountain forests Comparison of various algorithms for DTM interpolation from LIDAR data in dense mountain forests, *7254*. https://doi.org/10.5721/EuJRS20164932

Vivero, S., & Lambiel, C. (2019). Monitoring the crisis of a rock glacier with repeated UAV surveys. *Geographica Helvetica*, 59–69.

Yordanov, V., Fugazza, D., Azzoni, R. S., Cernuschi, M., Scaioni, M., Diolaiuti, G. A., … Imagery, S. (2019). Monitoring Alpine Glaciers from Close-Range To Satellite Sensors. *ISPRS*, *XLII*, 1803–1810.

Zemp, M., Haeberli, W., Hoelzle, M., & Paul, F. (2006). Alpine glaciers to disappear within decades ? *Geophysical Research Letters*, *Vol.33*, 4. https://doi.org/10.1029/2006GL026319

Appendix

Table 8 Displaying the resulting area and height measurements of the boulder on the glacier surface used for testing for what happens from point cloud to DEM interpolations

	Height and Area Measurements of Boulder Point Cloud and DEM Interpolations as Compared to the Actual Dimensions							
Data Type	TLS Area (m^2)	TLS Height (m)	Nadir Area (m^2)	Nadir Height (m)	Oblique Area (m^2)	Oblique Height (m)	Pix4D Area (m^2)	Pix4D Height (m)
Point Clouds	15.81	2.94	15.68	2.75	15.02	2.75	15.83	2.73
Binning Average Linear (25cm res.)	17.79	2.75	23.83	2.69	16.67	2.68	15.83	2.73
Binning Average Linear (15cm res.)	20.19	2.78	22.01	2.69	18.69	2.78	15.83	2.73
Binning Average Linear (5cm res.)	20.47	2.83	23.33	2.71	16.99	2.8	15.83	2.73
Binning IDW Linear (25cm res.)	17.6	2.86	20.06	2.72	17.23	2.69	15.83	2.73
Binning IDW Linear (15cm res.)	17.63	2.82	23.53	2.7	17.89	2.68	15.83	2.73
Binning IDW Linear (5cm res.)	18.36	2.83	21.66	2.74	17.48	2.76	15.83	2.73
Binning IDW NN (25cm res.)	18.36	2.75	21.39	2.69	17.6	2.68	15.83	2.73
Binning IDW NN (15cm res.)	17.61	2.86	23.45	2.73	17.67	2.71	15.83	2.73
Binning IDW NN (5cm res.)	16.71	2.87	19.85	2.66	17.91	2.77	15.83	2.73
Binning IDW Simple (25cm res.)	17.53	2.6	18.8	2.51	17.5	2.5	15.83	2.73
Binning IDW Simple (15cm res.)	18.87	2.46	n/a	2.54	16.9	2.56	15.83	2.73
Binning IDW Simple (5cm res.)	18.4	2.58	n/a	2.51	16.7	2.55	15.83	2.73
Triangulate Linear (25cm res.)	19.34	2.66	18.58	2.55	18.2	2.54	15.83	2.73
Triangulate Linear (15cm res.)	20.08	2.63	20.8	2.52	16.97	2.57	15.83	2.73
Tirangulate Linear (5cm res.)	20.36	2.58	21.6	2.54	17.2	2.62	15.83	2.73

Table 9 The averaged area measurements of a boulder on the surface of the glacier to test for differences in data collection method, data types, and DEM interpolations.

	Average Boulder Top Area Measurement of Each Method & Resolution (m^2)				
Data Type	TLS Area	Nadir Area	Oblique Area	Average	Actual
Point Clouds	15.81	15.68	15.02	15.50	15.83
Binning, Average, Linear	19.48	23.06	17.45	20.00	15.83
Binning, IDW, Linear	17.86	21.75	17.53	19.05	15.83
Binning, IDW, NN	17.56	21.56	17.73	18.95	15.83
Binning, IDW, Simple	18.27	18.8	17.03	18.03	15.83
Triangulate, Linear	19.48	20.33	17.46	19.09	15.83
Average (per collection method)	18.53	21.10	17.44		

Table 10 The averaged height measurements of a boulder on the surface of the glacier to test for differences in data collection method, data types, and DEM interpolations.

	Average Height Measurements of each Method & Resolution (m)				
Data Type	TLS Height	Nadir Height	Oblique Height	Average	Actual
Point Clouds	2.94	2.75	2.75	2.81	2.73
Binning, Average, Linear	2.79	2.70	2.75	2.75	2.73
Binning, IDW, Linear	2.84	2.72	2.71	2.76	2.73
Binning, IDW, NN	2.83	2.69	2.72	2.75	2.73
Binning, IDW, Simple	2.55	2.52	2.54	2.53	2.73
Triangulate, Linear	2.62	2.54	2.58	2.58	2.73
Average (per collection method	2.72	2.63	2.66		

Table 11 Statistical values of the M3C2 and DoD results at varying resolutions to be used for comparison

Change Statistics Comparison of M3C2 and DoD of Different DEM Interpolations

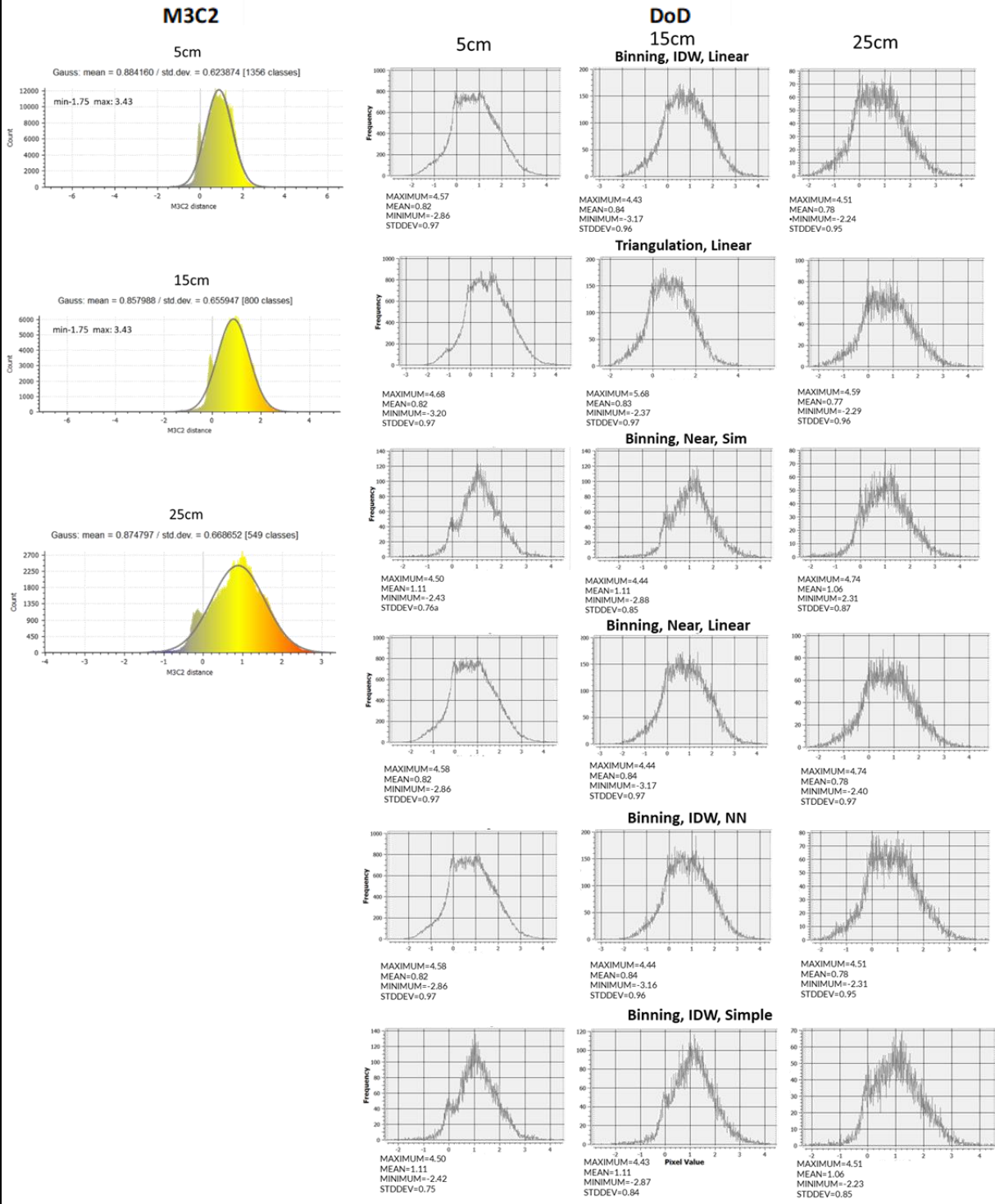| Data Format /Change Type	Mean	Standard Deviation	Maximum Increase	Maximum Decrease
Point Clouds M3C2 (<5cm res.)	0.844	0.624	3.43	-1.75
Point Clouds M3C2 (15cm res.)	0.858	0.656	3.43	-1.75
Point Clouds M3C2 (25cm res.)	0.875	0.669	3.43	-1.75
Binning, IDW, Linear (5cm res.)	0.82	0.97	4.57	-2.86
Binning, IDW, Linear (15cm res.)	0.84	0.96	4.43	-3.17
Binning, IDW, Linear (25cm res.)	0.78	0.95	4.51	-2.24
Triangulation, Linear (5cm res.)	0.82	0.97	4.68	-3.2
Triangulation, Linear (15cm res.)	0.83	0.97	5.68	-2.37
Triangulation, Linear (25cm res.)	0.77	0.96	4.59	-2.29
Binning, Near, Sim (5cm res.)	1.11	0.76	4.5	-2.43
Binning, Near, Sim (15cm res.)	1.11	0.85	4.44	-2.88
Binning, Near, Sim (25cm res.)	1.06	0.87	4.74	-2.31
Binning, Near, Linear (5cm res.)	0.82	0.97	4.58	-2.86
Binning, Near, Linear (15cm res.)	0.84	0.97	4.44	-3.17
Binning, Near, Linear (25cm res.)	0.78	0.97	4.74	-2.4
Binning, IDW, NN (5cm res.)	0.82	0.97	4.58	-2.86
Binning, IDW, NN (15cm res.)	0.84	0.96	4.44	-3.16
Binning, IDW, NN (25cm res.)	0.78	0.95	4.51	-2.31
Binning, IDW, Sim (5cm res.)	1.11	0.75	4.5	-2.42
Binning, IDW, Sim (15cm res.)	1.11	0.84	4.43	-2.87
Binning, IDW, Sim (25cm res.)	1.06	0.85	4.51	-2.23

Figure 29 Resulting histograms from the M3C2 and DoD change analysis results to see the distribution of the change values between methods. The M3C2 (left) providing results based on point clouds resampled to 5 cm, 15 cm, and 25 cm prior to processing the change. The DoD results (right) with each row representing a different interpolation method used and the columns being the resolution used when interpolating the DEMs before processing the change.